AD-A162 370 DELAMINATION BUCKLING AND GROWTH OF FLAT COMPOSITE STRUCTURAL ELEMENTS..(U) GEORGIA INST OF TECH ATLANTA SCHOOL OF ENGINEERING SCIENCE AN.. G J SIMITSES ET AL. 1/1

UNCLASSIFIED SEP 84 AFOSR-TR-85-1067 AFOSR-83-0243 F/G 20/11 NL

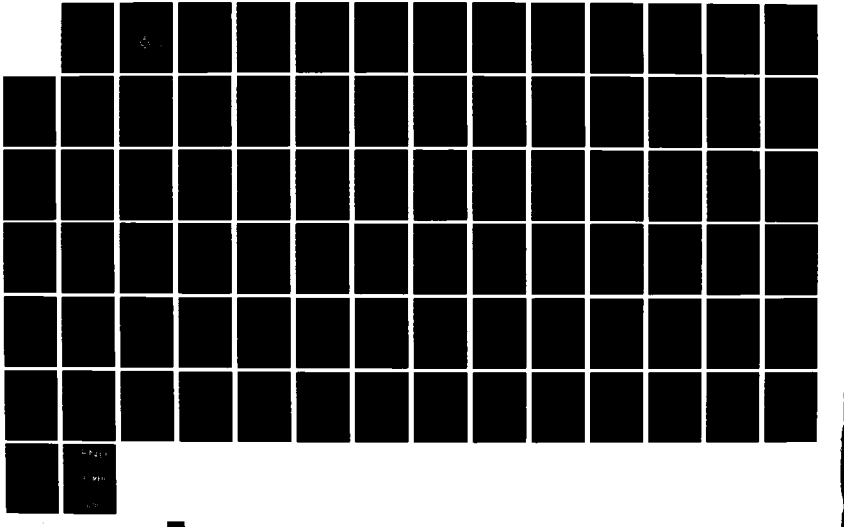

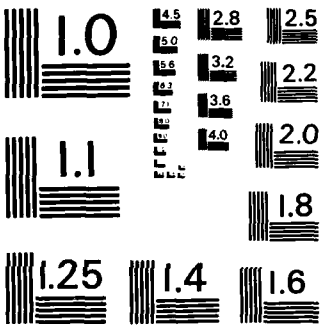

DELAMINATION BUCKLING AND GROWTH OF FLAT COMPOSITE STRUCTURAL ELEMENTS

by

George J. Simitses and Sayed Sallam

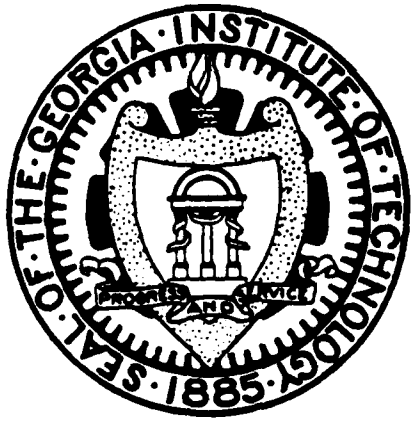

School of Engineering Science and Mechanics
GEORGIA INSTITUTE OF TECHNOLOGY
A Unit of the University System of Georgia
Atlanta, Georgia 30332

Unclassified

SECURITY CLASSIFICATION OF THIS PAGE (When Data Entered)

REPORT DOCUMENTATION PAGE	READ INSTRUCTIONS BEFORE COMPLETING FORM
1. REPORT NUMBER AFOSR-TR- 85-1007	2. GOVT ACCESSION NO. AD-A162 370
	3. RECIPIENT'S CATALOG NUMBER
4. TITLE (and Subtitle) DELAMINATION BUCKLING AND GROWTH OF FLAT COMPOSITE STRUCTURAL ELEMENTS	5. TYPE OF REPORT & PERIOD COVERED ~~FINAL~~ ANNUAL July 1, 1983 - August 31, 1984
	6. PERFORMING ORG. REPORT NUMBER
7. AUTHOR(s) George J. Simitses and S. Sallam	8. CONTRACT OR GRANT NUMBER(s) AFOSR 83-0243
9. PERFORMING ORGANIZATION NAME AND ADDRESS Georgia Institute of Technology School of Engineering Science and Mechanics 225 North Avenue S.W., Atlanta, GA 30332	10. PROGRAM ELEMENT, PROJECT, TASK AREA & WORK UNIT NUMBERS ~~61102F~~ 2307/B1 61102F
11. CONTROLLING OFFICE NAME AND ADDRESS AFOSR/NA Building 410 Bolling AFB, D.C. 20332	12. REPORT DATE September 1984
	13. NUMBER OF PAGES 80
14. MONITORING AGENCY NAME & ADDRESS(if different from Controlling Office)	15. SECURITY CLASS. (of this report)
	15a. DECLASSIFICATION/DOWNGRADING SCHEDULE

16. DISTRIBUTION STATEMENT (of this Report)

Approved for public release; distribution unlimited

17. DISTRIBUTION STATEMENT (of the abstract entered in Block 20, if different from Report)

18. SUPPLEMENTARY NOTES

19. KEY WORDS (Continue on reverse side if necessary and identify by block number)

Laminated Plates; Delamination Buckling; Delamination Growth; Damage Tolerance.

20. ABSTRACT (Continue on reverse side if necessary and identify by block number)

Delamination buckling and growth of flat composite structural elements is presented with sufficient detail. The mathematical model for the phenomena, are developed and solved. The emphasis of the analysis is to establish the load carrying capability (damage tolerance) of the delaminated structural element and to identify the most influencing structural parameters.

DD FORM 1 JAN 73 1473 EDITION OF 1 NOV 65 IS OBSOLETE

Unclassified

SECURITY CLASSIFICATION OF THIS PAGE (When Data Entered)

Two important parameters have a governing influence on the behavior of the delaminated (damaged) element: the size of the delamination and its position in the laminate, especially its distance from the surface. Depending on these two parameters, the damage tolerance of the laminate is either governed by (delamination) buckling or by the fracture toughness of the material (delamination growth).

DELAMINATION BUCKLING AND GROWTH OF FLAT COMPOSITE STRUCTURAL ELEMENTS*

by

George J. Simitses+ and Sayed Sallam++

School of Engineering Science and Mechanics
Georgia Institute of Technology, Atlanta, GA

* This work was supported by the United States Air Force Office of Scientific Research under Grant AFOSR-83-0243.

+ Professor and Principal Investigator

++ Graduate Research Assistant.

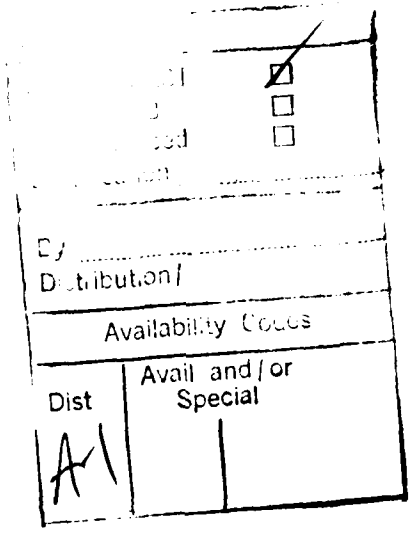

TABLE OF CONTENTS

NOMENCLATURE

a	length of delamination
h	thickness of delaminations
ℓ_1	distance of delamination from left end of the plate
t	thickness of the plate
L	length of the plate
H	$= t - h$
$\bar{\ }$	$= a/L$
$\bar{h}$	h/t
$\bar{a}_{ij}$, $\bar{C}_{ij}$	constants
A_{xx}, C_{xx}	axial stretching stiffness
B_{xx}	coefficient of coupling between bending and stretching
D_{xx}	axial bending stiffness
Q_{xx}	axial stiffness of single layer
E_{xx}, E_{yy}, ν_{xy}	material constants
P_i	axial forces
$\bar{P}_i = -P_i$	applied compressive forces
k_i^2	$= \dfrac{\bar{P}_i}{\left(D_{xx} - \dfrac{B_{xx}^2}{A_{xx}}\right)_i}$
M_i	bending moments
N_{xx}	stress resultant
V_i	shear forces
u_i	in-plane displacements

w_i transverse displacements

G energy release rate

$\overline{G}$ $= G \dfrac{L^4}{Q_{xx}\, t^5}$

G^* critical value of G

$\overline{G}^*$ $= G^* \dfrac{L^4}{Q_{xx}\, t^5}$

$(\ )^P$ Primary state parameters

$(\ )^a$ additional state parameters

SUMMARY

This report summarizes the first year work under the general heading of "Effect of Local Material Imperfections on the Buckling Behavior of Composite Structural Elements".

It describes, through the introduction, two important areas: one of delamination buckling and growth and one of the holes and foreign inclusions.

In the subsequent sections, the important subject of delamination buckling and delamination growth is presented with sufficient detail. The geometries considered are flat laminates and the emphasis is to establish the load carrying capability (damage tolerance) of the laminate. It is clearly shown that two important parameter govern the behavior of the delaminated (damaged) laminate: the size of the delamination and its position (especially relative to its distance from the surface). Depending on these two parameters the damage tolerance of the laminate is either governed by buckling or by the fracture toughness of the material (delamination growth). Finally, the second year effort is described. This includes the analysis of delaminated cylindrical shells under various load conditions.

I. INTRODUCTION

The constant demand for lighter and more efficient structural configurations has led the structural engineer to the use of new man-made materials. At the same time this demand forced upon him very sophisticated methods of testing, analysis and design, as well as of fabrication and manufacturing. The recent explosive progress in producing and using composite materials has pointed towards the clear possibility of man creating specific materials for specific missions. At the same time it has been realized that some severe needs are created (related to this effort) namely (i) the complete understanding of the behavior of composite materials and what influences this behavior, (ii) the establishment of design criteria upon which proper use of composites rests, and (iii) the training of engineers in the area of composite structures. In all three items, it is important to recognize that, with the advent of composite media, certain new material imperfections, can be found in composite structures as well as the better known imperfections, that one finds in metallic structures. Thus, broken fibers, delaminated regions, cracks in the matrix material as well as holes, foreign inclusions and small voids constitute material and structural imperfections that do exist in composite structures.

I.1 Delamination Buckling and Growth (Flat Plates)

One of the most common failure modes in composite materials is delamination.

Delamination is developed as a result of imperfections in the production technology or due to the effect of certain factors during the operational life of the laminate, such as impact by foreign objects. The presence of delamination in a laminated composite material may cause local

buckling and reduction in the over-all stiffness of the structure, which may lead to early failure.

Problems of delamination growth in composites have recieved attention in recent years.

A double cantilever beam (D C B) specimen loaded in compression was used by Chow & Ngan (1) to study the effect of buckling on crack propagation. Initial geometric imperfection was made in the specimen in order to obtain crack propagation at loads below the buckling load of the perfect column. Chai (2) carried out an experimental program to determine the damage propagation mechanisms of a composite panel (graphite/epoxy) under simultaneous compressive in-plane loading and low-velocity transverse impact. Also, he presented an analytical (one-dimensional) model for delamination buckling and damage growth. For a homogeneous isotropic plate under a compressive displacement-controlled loading, he obtained a closed form expression for the energy release rate for the case of a thin film model (the buckling of the delaminated layer assumed to produce a negligible bending deformation in the main body of the laminate). A more general model, where the delamination thickness was of the same order of magnitude as the other thicknesses involved, was also considered.

Whitcomb (3) presented an approximate analysis for a symmetric through-width delamination of a unidirectional graphite/epoxy bonded to an aluminum bar. The buckled region was assumed to have zero slope at both ends. For the case of short and thick delaminated regions, the rotations at the ends cannot be neglected, hence he accounted for the rotations by considering a modified delaminatin length (effective length) which he obtained through a finite element solution of the postbuckling problem.

A finite element stress analysis was developed (4) to study the postbuckling behavior. The stress distribution and strain energy release rate were calculated for various delamination lengths, delamination depths, applied loads and lateral deflections. A few specimens, consisting of unidirectional graphite/epoxy bonded to aluminum, were fatigue-tested to obtain delamination growth data. Yin and Wang (5) derived a simple expression for the energy release rate associated with the growth of a general one-dimensional delamination. First, a continuous stress field produced by a certain subsystem of forces and moments was eliminated, then the energy release rate associated with the remaining system of forces and moments was evaluated by means of the path-independent J-integral. Also, they (5) studied the possibilit of cracks branching off to neighboring interlaminar faces and the condition for coalescing of multiple parallel delaminations into a single layer.

A two-dimensional model, consisting of an internal rectangular delamination with initial displacement imperfection in the thinner portion, was proposed by Konishi (6). A test program was carried on a hybrid specimen, boron/graphite/epoxy covers, and graphite/epoxy substructure. The effect of static and cyclic loading on delamination growth was studied. Moreover, the effects of temperature and moisture were taken into consideration.

The case of a circular homogeneous isotropic plate with a concentric penny-shaped delaminatin subject to a radial compressive loading was addressed in refs. (7-9). Based on an asymptotic analysis of the postbuckling behavior of the delaminate layers, Bottega and Maewal (8) considered the case of symmetric split, where the delaminatin assumed to exist and grow in the mid-plane of the laminate. Considering

time-dependent loading and taking into account the inertia of the delaminated layers, Bottega and Maewal (9) examined the dynamics of the growth of penny-shaped delamination in a circular plate. The load applied was in the form of a radial compressive load and a distributed transverse tensile pulse. Using Hamilton's principle the equations of motion and the corresponding growth laws were derived. Two models were studied by Yin (7) concerning the delamination buckling of a penny-shaped delamination, the thin film model and the symmetric split model. The energy release rate was obtained for both models (7) by means of the M-integral.

Using finite element and Rayleigh-Ritz methods Shivakumar and Whitcomb (10) predicted the buckling behavior of an elliptic delamination embedded near the surface of a thick quasi-isotropic laminate. The laminate was symmetric made of graphite/epoxy laminae. The results obtained by using Rayleigh Ritz analysis showed good agreement with those obtained by using finite element methods, except for highly anisotropic sublaminates.

The present work deals primarily with the question of delamination buckling and growth and how the presence of the delamination affects the global load carrying capacity of the system. A one-dimensional model is presented in order to predict (a) delamination buckling loads of across the width delaminated, axially loaded laminated plate and (b) the ultimate load-carrying capability of above geometry, when delamination growth takes place. The model is employed to predict critical loads for delaminated wide columns with both simply supported and clamped ends. The effects of delamination position, size and thickness on the critical loads are studied in detail for both sets of boundary conditions. Results are obtained for delaminated isotropic plates and for plates made up of special type of symmetric cross-ply laminates. The results reveal that for certain

geometries the buckling load can serve as a measure of the load carrying capacity of the delaminated configuration. In other cases, the buckling load is very small and delamination growth is strong possibility, depending on the toughness of the material. Also, the present model can be used to study the effect of the presence of coupling between bending and stretching on delamination growth. In this aspect, a delaminated plate in the form of unsymmetric cross-ply laminate is studied.

I.2 Effect of Holes and Foreign Inclusions on Buckling

The effect of small cutouts of various shapes on the response of elastc shells has received great attention. Experimental studies have shown that holes could cause a severe reduction in the buckling loads of shells.

Based ona two-dimensional finite difference scheme, Brogan and Almroth (11) presented a nonlinear analysis for cylindrical shells with rectangular cutouts. A modified Newton method was used (11) to reduce the computational time. Also, simple experiments were performed (11) in order to verify the computational scheme and satisfactory agreement between the theory and test were obtained. A finite element analysis of a cylindrical shell with reinforced circular opening was presented by Meller and Bushnell (12). The cylindrical shell was ring-stiffened and made of steel, and axially compressed. The effect of geometric imperfection was included (12). At the same time, a similar work to that done by Mellar was carried out by Baker and Bennett (13). They (13) tested a ring-stiffened cylindrical shell, reinforced with circular holes under the action of unsymmetric axial loading. The effect of hole diameter on the buckling load was reported (13). Also, they (13) took into consideration when the penetrations

(holes) were cutting no ring stiffeners, and cutting one, two and three ring-stiffeners.

As far as the effect of small holes on composite structure is concerned, an experimental program was carried out by Byers (14) on a damaged graphite/polymer laminate. A controlled damage in the form of circular holes and simulated delamination were introduced into the composite specimens (14), which were subjected to static compression and cyclic compression load. Four different types of graphite/polymer were tested to evaluate the damage tolerance of each type. In some cases the compression strength of the damaged specimens reduced to 40% of the compression strength of the undamaged specimens.

Another material imperfection is the rigid inclusion (small). The effect of rigid inclusions on the stress field of the medium in the neighborhood of the inclusion has received (limited) attention in the past 25 years [15-19]. As far as these authors know, the effect of rigid inclusions on the buckling characteristics of the system (that contains the rigid inclusion) has not been studied.

I.3 Future Work

The problem of buckling of delaminated cylindrical shells has not received the deserved attention. Very few investigations have been carried out in this area. Kulkarni and Frederic (20) used a "branched integration" technique to solve the problem of buckling of two layered cylindrical shell, partially debonded, subjected to axial compression. They (20) considered the case where the delamination originates at the boundary. Results were obtained for different lengths of debonding and inner to outer layer thickness ratios. A significant decrease in the critical load was observed. The buckling of stiffened circular cylindrical shells, with two

unbonded orthotropic layers, was reported by Jones (21). Jones (21) assumed that the layers did not separate during buckling, i.e. the deformation of both layers were assumed to be the same. Also, he examined the case where one of the two unbonded orthotropic layers was circumferentially cracked. His results for a cylindrical shell made of aluminum with ablative outer layer subjected to hydrostatic pressure showed that the ablative layer had to be increased by 50% in thickness in the damaged (unbonded) cylindrical shell in order to obtain the same buckling loads of the perfect cylindrical shell. Troshin (22) examined the effect of longitudinal delamination in a laminar cylindrical shell in the critical external pressure. The delamination was assumed to extend over the entire length of the shell. He studied the effect of the length and position of the delamination over the shell thickness on the critical external pressure.

It is intended to extend the one-dimensional model of sectin (I) to a two-dimensional model to investigate and study the effect of circumferential delamination on the buckling loads of circular cylindrical shells subject to compressive loading. Other delamination shapes and loads will also be considered.

II. MATHEMATICAL FORMULATION

II.1 Description of the Problem

A one-dimensional modelling of the laminated plate is employed. This is similar to the one used in Ref. 3.

Delamination exists and grows (if it does) along a plane parallel to the reference plane. This simplified modelling is employed in order to understand better and pay more attention to the physical behavior, rather than get involved (and lost) in a more complex model with several additional parameters and a considerably more difficult solution scheme. In accordance with this philosophy, it is also assumed that the delamination exists before the compressive loading is applied. The location and length (size) of the delamination is arbitrary and the ends of the plate are either hinged or clamped (see Fig. 1). Note that, because of the one-dimensional modelling, the sides of the plate are free. Finally, it is assumed that the delamination separates the column (or plate) into four regions, and each one of these regions has such dimensions (lengths and thicknesses) that Euler-Bernoulli beam theory is applicable (this assumption may also be removed by employing more accurate theories for small length to thickness ratios).

The three axes of orthotropy are parallel to the reference frame x,y,z. The natural plane of the plate lies on the xy-plane. The plate is of unit width and is subjected to a uniform compressive load, $\bar{P}$, along the supported edges. A layer of uniform but arbitrary thickness h and of length a is delaminated (see Fig. 1). The delamination extends across the entire width of the plate (one-dimensional modelling). Note from Fig. 1 that the delamination divides the plate (column) into four regions, 1-4. The coordinate system is such that $\underline{x}$ is measured from the left end.

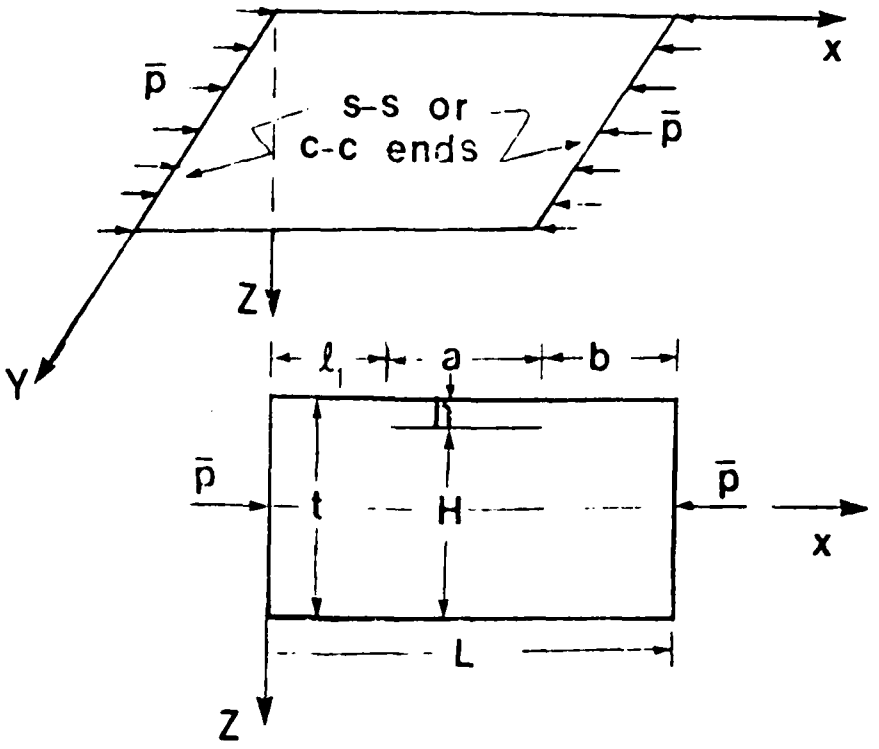

Fig. 1. Geometry, Loading and Sign Convention

Moreover, u_i and w_i ($i = 1,2,3,4$) denote the in-plane and transverse displacements of material poins on the midplane of each region (each part). For example, w_3 is the transverse displacement of material points on the plane h/2 units from the top surface (region 3), while w_2 is the transverse displacement of material points on the plane H/2 units from the bottom surface (region 2). Furthermore, note that because of the Euler-Bernoulli assumptions $w_i(x)$ characterizes the transverse displacement of every material point in region i and position x. Similarly, the inplane displacement, $\bar{u}_i(x,z_i)$, of every material point is given by

$$\bar{u}_i(x, z_i) = u_i(x) - z_i w_{i,x} \qquad (1)$$

where z_i is measured from the midsurface of each region and the comma denotes differentiation with respect to the index that follows.

II.2 *Delamination Buckling*

The delaminated plate (wide column) is assumed to be:

(a) homogeneous and, at most, orthotropic or

(b) made up of special type of symmetric cross-ply laminates; such that the prebuckling state is a membrane one.

The necessary equations, including kinematic relations, constitutive relations, relations between loads and moments on one side and kinematic parameters on the other, and equilibrium equations, are given below:

$$\varepsilon_{xx_i} = \varepsilon^0_{xx_i} - z_i w_{i,xx}$$

$$\varepsilon^0_{xx_i} = u_{i,x} + \frac{1}{2} w^2_{i,x} \qquad (2)$$

$$N_{xx_i} = C_{xx_i} \varepsilon^0_{xx_i} \qquad (3)$$

$$M_{xx_i} = -D_{xx_i} W_{i,xx} \tag{4}$$

$$V_i = -(D_{xx_i} W_{i,xx})_{,x} + N_{xx_i} W_{i,x} \tag{5}$$

$$P_{i,x} = 0 \tag{6}$$

$$(D_{xx_i} W_{i,xx})_{,xx} - P_i W_{i,xx} = 0 \tag{7}$$

where

P_i axial forces

M_i bending moments

V_i shearing force

Note that: for our problem (unit width plate)

$$N_{xx_i} = P_i$$

where

$$C_{xx_i} = \begin{cases} A_{xx_i} & \text{if } \varepsilon_{yy} \equiv 0 \text{ (plate strip)} \\ \left(A_{xx} - \frac{A_{xy}^2}{A_{yy}}\right)_i & \text{if } \sigma_{yy} \equiv 0 \text{ (wide column)} \end{cases} \tag{8}$$

$$A_{IJ} = \sum_{k=1}^{n} Q^k_{IJ_i} (h_k - h_{k-1}) \qquad I, J = x, y \quad i = 1,2,3,4 \tag{9}$$

$$D_{xx_i} = \frac{1}{3} \sum_{k=1}^{n} Q^k_{xx} (h_k^3 - h_{k-1}^3) \tag{10}$$

$$[Q]^k = \begin{bmatrix} \frac{E_{xx}}{1-\nu_{xy}\nu_{yx}} & \frac{\nu_{xy}E_{yy}}{1-\nu_{xy}\nu_{yx}} & 0 \\ \frac{\nu_{yx}E_{xx}}{1-\nu_{xy}\nu_{yx}} & \frac{E_{yy}}{1-\nu_{xy}\nu_{yx}} & 0 \\ 0 & 0 & G_{xy} \end{bmatrix}^k \qquad (11)$$

$E^k_{xx_i}$, $E^k_{yy_i}$, $\nu^k_{xy_i}$ & $G^k_{xy_i}$ material Constants of laminate (k) in plate (i)

The boundary conditions, both in-plane and transverse and the continuity conditions (kinematic and internal loads) are also listed below:

In-Plane Boundary Conditions:

$$\text{at } x=0: u_1=0 \;;\; \text{at } x=L: P_4=-\bar{P} \qquad (12)$$

Transverse Boundary Conditions:

(a) Simple Suppports,

at x = 0: $w_1 = 0$ and $w_{1,xx}=0$

at x = L: $w_4 = 0$ and $w_{4,xx}=0$ (13a)

(b) Clamped Supports

at x = 0: $w_1 = 0$ and $w_{1,x}=0$

at x = L: $w_4 = 0$ and $w_{4,x}=0$ (13b)

Kinematic Continuity Conditions

at $x=\ell_1$:

$$u_1 - \frac{h}{2}w_{1,x} = u_2$$

$$u_1 + \frac{H}{2}w_{1,x} = u_3 \qquad (14a)$$

$$w_1 = w_2 = w_3$$

$$w_{1,x} = w_{2,x} = w_{3,x}$$

at $x = \ell_1 + a$:

$$u_4 - \frac{h}{2} w_{4,x} = u_2$$

$$u_4 + \frac{H}{2} w_{4,x} = u_3$$

$$w_4 = w_2 = w_3 \qquad (14b)$$

$$w_{4,x} = w_{2,x} = w_{3,x}$$

Continuity in Moments and Forces

at $x = \ell_1$:

$$M_1 - M_2 - M_3 + P_3 \frac{H}{2} - P_2 \frac{h}{2} = 0$$

$$-V_1 + V_2 + V_3 = 0 \qquad (15a)$$

$$-P_1 + P_2 + P_3 = 0$$

at $x = \ell_1 + a$:

$$M_4 - M_2 - M_3 + P_3 \frac{H}{2} - P_2 \frac{h}{2} = 0$$

$$-V_4 + V_2 + V_3 = 0 \qquad (15b)$$

$$-P_4 + P_2 + P_3 = 0$$

where M_i, V_i and P_i can be expressed in terms of the displacement gradients, through Eqs. (2) to (7).

II.2.1 Primary (Membrane) State Solution

As the compressive load P is applied (quasi) statically, the plate remains flat and a primary state solution is characterized by

$$W_i^P = 0$$
$$\text{and} \quad u_i^P = \bar{A}_i x + \bar{B}_i \tag{16}$$

where $\bar{A}_i$ and $\bar{B}_i$ are arbitrary constants.

Use of the boundary and continuity conditions leads to complete knowledge of the primary state, or

$$W_i^P \equiv 0 \qquad i = 1,2,3,4$$
$$u_i^P = \frac{P_i^P}{C_{xx_i}} x \qquad i = 1,2,3,4 \tag{17}$$

and

$$P_1^P = P_4^P = -\bar{P} \; ;$$
$$P_2^P = -\frac{C_{xx_2}}{C_{xx_1}} \bar{P} \quad ; \quad P_3^P = -\frac{C_{xx_3}}{C_{xx_1}} \bar{P} \tag{18}$$

$$M_i^P = 0$$
$$V_i^P = 0 \qquad i = 1,2,3,4 \tag{19}$$

II.2.2 Buckling Equations

The buckling equations are derived by method[23-25], based on the concept of the e equilibrium position at a bifurcation point required steps are as follows: start with the proper boundary and interior continuity con purturb them (from the primary state) by allo admissable changes in the displacement functio at a point at which an adjacent equilibrium pa point), and retain first-order terms in the a resulting linear ordinary differential equations a The corresponding boundary and continuity condi pururbation technique.

The following expressions are substituted in e

$$u_i = u_i^P + u_i^a \quad ; \quad w_i = w_i^a$$

$$P_i = P_i^P + P_i^a$$

$$M_i = M_i^a \quad ; \quad V_i = V_i^a$$

where the super "a" parameters denote the small a correspond to the admissible variation w_i^a and u_i^a).

The buckling equations are:

$$P_{i,x}^a = 0$$

$$D_{xx_i} w_{i,xxxx}^a - P_i^P w_{i,xx}^a = 0$$

The related conditions are

In-Plane Boundary Conditions

$$\text{at } x=0: \quad u_1^a = 0 \;; \text{ at } x=L: \quad P_4^a = 0 \qquad (23)$$

Transverse Boundary Conditions

(a) Simple Supports

$$\begin{aligned} &\text{at } x=0: \quad w_1^a = 0 \text{ and } w_{1,xx}^a = 0 \\ &\text{at } x=L: \quad w_4^a = 0 \text{ and } w_{4,xx}^a = 0 \end{aligned} \qquad (24a)$$

(b) Clamped Supports

$$\begin{aligned} &\text{at } x=0: \quad w_1^a = 0 \text{ and } w_{1,x}^a = 0 \\ &\text{at } x=L: \quad w_4^a = 0 \text{ and } w_{4,x}^a = 0 \end{aligned} \qquad (24b)$$

Kinematic Continuity Conditions

$$\begin{aligned} &\text{at } x=\ell_1: \\ &\qquad u_1^a - \frac{h}{2} w_{1,x}^a = u_2^a \\ &\qquad u_1^a + \frac{H}{2} w_{1,x}^a = u_3^a \\ &\qquad w_1^a = w_2^a = w_3^a \\ &\qquad w_{1,x}^a = w_{2,x}^a = w_{3,x}^a \end{aligned} \qquad (25a)$$

$$\begin{aligned} &\text{at } x=\ell_1+a \\ &\qquad u_4^a - \frac{h}{2} w_{4,x}^a = u_2^a \\ &\qquad u_4^a + \frac{H}{2} w_{4,x}^a = u_3^a \\ &\qquad w_4^a = w_2^a = w_3^a \\ &\qquad w_{4,x}^a = w_{2,x}^a = w_{3,x}^a \end{aligned} \qquad (25b)$$

Continuity in Moments and Forces

at $x = \ell_1$

$$M_1^a - M_2^a - M_3^a + P_3^a \frac{H}{2} - P_2^a \frac{h}{2} = 0$$

$$-V_1^a + V_2^a + V_3^a = 0 \qquad (26a)$$

$$-P_1^a + P_2^a + P_3^a = 0$$

at $x = \ell_1 + a$

$$M_4^a - M_2^a - M_3^a + P_3^a \frac{H}{2} - P_2^a \frac{h}{2} = 0$$

$$-V_4^a + V_2^a + V_3^a = 0 \qquad (26b)$$

$$-P_4^a + P_2^a + P_3^a = 0$$

.2.3 Solution of Buckling Equations

The solution to the buckling equations can be written as

$$U_i^a = \bar{C}_{i1} x + \bar{C}_{i2} \qquad (27a)$$

$$W_i^a = a_{i1} \sin k_i x + a_{i2} \cos k_i x + a_{i3} x + a_{i4}$$

where $k_i^2 = -\left(P_i^P / D_{xx_i}\right)$ $\qquad (27b)$

$i = 1, 2, 3, 4$

P_i^P are given by Eqs (18)

Note that, since the admissible variations in the displacement components can be made as small as one wishes, the reference surface strain can be linearized, or (see Eq. (2)).

$$(\varepsilon^{o}_{xx_i})^{a} = u^{a}_{i,x} \tag{28}$$

Thus, the expressions for the internal forces and moments become (see Eqs. (3-5).

$$\begin{aligned} P_i^a &= C_{xx_i}\, u^a_{i,x} \\ M_i^a &= -D_{xx_i}\, w^a_{i,xx} \\ V_i^a &= -D_{xx_i}\, w^a_{i,xxx} + P_i^P\, w^a_{i,x} \end{aligned} \tag{29}$$

Moreover, the solution to the buckling equations, Eqs. (27), requires knowledge of 24 constants ($\bar{C}_{i1}$, $\bar{C}_{i2}$, a_{ij}, i = 1,2,3,4 and j = 1,2,3,4). There exist 24 boundary and continuity conditions, which are homogeneous in u_i, w_i and their space-derivatives. These consist of two in-plane boundary conditions, Eqs. (23), four transverse boundary conditions, either Eqs. (24a) or Eqs. (24b), twelve kinematic continuity conditions, Eqs. (25a) and (25b), and six continuity conditions in moments and forces, Eqs. (26a) and (26b). Their number is 24 also.

Use of the boundary conditions yields a system of linear, homogeneous, algebraic equations in $\bar{C}_{i1}$, $\bar{C}_{i2}$ and a_{ij}. For a nontrivial solution to exist the determinant of the coefficients must vanish. The determinant contains geometric parameters and the applied load $\bar{P}$, because of the presence of P_i^P [see Eqs. (18)].

Before proceeding with the description and actual solution of the determinant, certain non-dimensionalized parameters are introduced. These are

$$\bar{a} = \frac{a}{L} \; ; \; \bar{h} = \frac{h}{t} \; ; \; \bar{H} = \frac{H}{t} = 1 - \bar{h}$$

$$\bar{P} = \frac{\bar{P}}{P_{cr_{perf.}}} \; ;$$

$$P_{cr_{perf.}} = \begin{cases} \dfrac{\pi^2 D_{xx_1}}{L^2} & \text{for S-S} \\ \dfrac{4\pi^2 D_{xx_1}}{L^2} & \text{for C-C} \end{cases} \qquad (30)$$

$$\bar{P}_3 = \frac{\bar{P}_3}{P_{thin}} \; ; \; P_{thin} = \frac{4\pi^2 D_{xx_3}}{a^2}$$

$$P_3^a = \frac{P_3^a}{P_{thin}}$$

$$K_{ij} = K_i \, \ell_j \qquad i = 1, 2, 3, 4 \; ; \; j = 1, 2, 3 \qquad (31)$$

where $K_i^2 = -\dfrac{P_i^P}{D_{xx_i}}$

$$\ell_1 = \ell_1$$
$$\ell_2 = \ell_1 + a$$
$$\ell_3 = L$$

Note: for the considered case, where all four regions (plates) are symmetric w.r.t. their mid-reference planes, the following relations holds:

$$\frac{C_{xx_2}}{C_{xx_1}} = \bar{H} \quad ; \quad \frac{C_{xx_3}}{C_{xx_1}} = \bar{h}$$

hence $$k_2 = D_{21} k_1 \quad ; \quad k_3 = D_{31} k_1 \quad ; \quad k_4 = D_{41} k_1 \qquad (32)$$

where

$$D_{21} = \sqrt{(1-\bar{h})\ \frac{D_{xx_1}}{D_{xx_2}}}$$

$$D_{31} = \sqrt{\bar{h}\ \frac{D_{xx_1}}{D_{xx_3}}}$$

$$D_{41} = 1$$

Now, we can write the following expressions for the k_{ij}'s

$$K_{13} = 2\pi\sqrt{\bar{P}}$$

$$K_{12} = (\bar{\ell}_1 + \bar{a})\, K_{13} \qquad (33)$$

$$K_{11} = \bar{\ell}_1\, K_{13}$$

& $$k_{ij} = D_{i1}\, k_{1j} \qquad \begin{matrix} i = 2,3,4 \\ j = 1,2,3 \end{matrix} \qquad (34)$$

let $$Dc = \frac{D_{xx_3}}{h^2 C_{xx_3}} \qquad (35)$$

Moreover, the nondimensionalized coefficients $\bar{a}_{ij}$, are defined as

$$\bar{a}_{ij} = a_{ij}/t \qquad \begin{matrix} i=1,2,3,4 \\ j=1,2,4 \end{matrix} \qquad (36a)$$

$$\bar{a}_{i3} = a_{i3}L/t \qquad i=1,2,3,4 \qquad (36b)$$

In terms of the new non-dimensionalized quantities, the system of homogeneous, linear algebraic equations which govern the buckling of the delaminated plate, could be written as:

$$[A]\{X\} = 0 \qquad (37)$$

where [A] is a twenty by twenty matrix and {X} a one by twenty (column) matrix.

$$\{X\}^T = \{\bar{a}_{11}\ \bar{a}_{12}\ \bar{a}_{13}\ \bar{a}_{14}\ \bar{a}_{21}\ \bar{a}_{22}\ \bar{a}_{23}\ \bar{a}_{24}\ \bar{a}_{31}\ \bar{a}_{32}\ \bar{a}_{33}\ \bar{a}_{34}\ \bar{a}_{41}\ \bar{a}_{42}\ \bar{a}_{43}\ \bar{a}_{44}\ \bar{c}_{22}\ \bar{c}_{32}\ \bar{c}_{42}\ \bar{P}_3^a\} \qquad (38)$$

For a nontrivial solution to exist for the system of Eqs. (37), the determinant of the coefficients must vanish (see Eq. 39). The lowest eigenvalue ($\bar{P}$) gives the value of the critical load. Note that the elements of the determinant in Eq. (39) contain the geometric parameters $\bar{h}$, $\bar{\ell}$ and $\bar{a}$ as well as the material parameters, E_{xx}, E_{yy}, ν_{xy}, the effect of stacking sequence included in D_{xx_i}, load parameter $\bar{P}$.

I.3 Delamination Growth

Delamination of a composite laminate reduces the over-all stiffness and thereby lowers the buckling load of the laminate. The latter may or

$$A = \begin{vmatrix}
0 & 0 & 0 & 0 & -.5\bar{h}\,k_{23}\cos k_{21} & .5\bar{h}\,k_{23}\sin k_{21} & -.5\bar{h} & 0 & 0 & 0 \\
0 & 0 & 0 & 0 & 0 & 0 & 0 & 0 & .5\bar{H}\,k_{33}\cos k_{31} & -.5\bar{H}\,\epsilon_{33}\sin \\
\sin k_{11} & \cos k_{11} & \bar{I}_1 & 1 & -\sin k_{21} & -\cos k_{21} & -\bar{I}_1 & -1 & 0 & 0 \\
\sin k_{11} & \cos k_{11} & \bar{I}_1 & 1 & 0 & 0 & 0 & 0 & -\sin k_{31} & -\cos \\
k_{13}\cos k_{11} & -k_{13}\sin k_{11} & 1 & 0 & -k_{23}\cos k_{21} & k_{23}\sin k_{21} & -1 & 0 & 0 & 0 \\
k_{13}\cos k_{11} & -k_{13}\sin k_{11} & 1 & 0 & 0 & 0 & 0 & 0 & -\epsilon_{33}\cos k_{31} & k_{33}\sin \\
0 & 0 & 0 & 0 & -.5\bar{h}\,k_{23}\cos k_{22} & .5\bar{h}\,k_{23}\sin k_{22} & -.5\bar{h} & 0 & 0 & 0 \\
0 & 0 & 0 & 0 & 0 & 0 & 0 & 0 & .5\bar{H}\,k_{33}\cos k_{32} & -.5\bar{H}\,k_{33}\sin \\
0 & 0 & 0 & 0 & -\sin k_{22} & -\cos k_{22} & -(\bar{I}_1+\bar{a}) & -1 & 0 & 0 \\
0 & 0 & 0 & 0 & 0 & 0 & 0 & 0 & -\sin \epsilon_{32} & -\cos \\
0 & 0 & 0 & 0 & -k_{23}\cos k_{22} & k_{23}\sin k_{22} & -1 & 0 & 0 & 0 \\
0 & 0 & 0 & 0 & 0 & 0 & 0 & 0 & -k_{33}\cos k_{32} & k_{33}\sin k \\
\sin k_{11} & \cos k_{11} & 0 & 0 & -\bar{H}\sin k_{21} & -\bar{H}\cos k_{21} & 0 & 0 & -\bar{h}\sin k_{31} & -\bar{h}\cos \\
0 & 0 & -1 & 0 & 0 & 0 & \bar{H} & 0 & 0 & 0 \\
0 & 0 & 0 & 0 & -\bar{H}\sin k_{22} & -\bar{H}\cos k_{22} & 0 & 0 & -\bar{h}\sin k_{32} & -\bar{h}\cos \\
0 & 0 & 0 & 0 & 0 & 0 & \bar{H} & 0 & 0 & 0 \\
0 & 1 & 0 & 1 & 0 & 0 & 0 & 0 & 0 & 0 \\
\underline{k_{13}} & \underline{0} & \underline{1} & 0 & 0 & 0 & 0 & 0 & 0 & 0 \\
0 & 0 & 0 & 0 & 0 & 0 & 0 & 0 & 0 & 0 \\
0 & 0 & 0 & 0 & 0 & 0 & 0 & 0 & 0 & 0
\end{vmatrix}$$

In case of s-s boundaries, the underlined terms have to be changed to:

A(18,1) = 0.0
A(18,2) = 1.0
A(18,3) = 0.0

A(20,13) = sin k_{13}
A(20,14) = cos k_{13}
A(20,15) = 0.0

182

$$
\begin{array}{cccccccccccc}
0 & 0 & 0 & 0 & 0 & 0 & 0 & 1 & 0 & 0 & -4\pi^2\,\bar{h}^3 De\,\bar{I}_1/\bar{H}\,\bar{a}^2 \\
-.5\bar{h}\,k_{33}\sin k_{31} & .5\bar{H} & 0 & 0 & 0 & 0 & 0 & 0 & 1 & 0 & 2\pi^2\,\bar{h}^2 De\,\bar{I}_1/\bar{a}^2 \\
0 & 0 & 0 & 0 & 0 & 0 & 0 & 0 & 0 & 0 & 0 \\
-\cos k_{31} & -\bar{I}_1 & -1 & 0 & 0 & 0 & 0 & 0 & 0 & 0 & 0 \\
0 & 0 & 0 & 0 & 0 & 0 & 0 & 0 & 0 & 0 & 0 \\
k_{33}\sin k_{31} & -1 & 0 & 0 & 0 & 0 & 0 & 0 & 0 & 0 & 0 \\
0 & 0 & 0 & 0 & 0 & 0 & 0 & 1 & 0 & -1 & -4\pi^2\,\bar{h}^3 De\,(\bar{I}_1+\bar{a})/\bar{H}\,\bar{a}^2 \\
-.5\bar{h}\,k_{33}\sin k_{32} & .5\bar{H} & 0 & 0 & 0 & 0 & 0 & 0 & 1 & -1 & 4\pi^2\,\bar{h}^2 De\,(\bar{I}_1+\bar{a})/\bar{a}^2 \\
0 & 0 & 0 & \sin k_{12} & \cos k_{12} & (\bar{I}_1+\bar{a}) & 1 & 0 & 0 & 0 & 0 \\
-\cos k_{32} & -(\bar{I}_1+\bar{a}) & -1 & \sin k_{12} & \cos k_{12} & (\bar{I}_1+\bar{a}) & 1 & 0 & 0 & 0 & 0 \\
0 & 0 & 0 & k_{13}\cos k_{12} & -k_{13}\sin k_{12} & 1 & 0 & 0 & 0 & 0 & 0 \\
k_{33}\sin k_{32} & -1 & 0 & k_{13}\cos k_{12} & -k_{13}\sin k_{12} & 1 & 0 & 0 & 0 & 0 & 0 \\
-\bar{h}\cos k_{31} & 0 & 0 & 0 & 0 & 0 & 0 & 0 & 0 & 0 & -2\pi^2\,\bar{h}/\bar{a}^2\,k_{33}^2 \\
0 & \bar{h} & 0 & 0 & 0 & 0 & 0 & 0 & 0 & 0 & 0 \\
-\bar{h}\cos k_{32} & 0 & 0 & \sin k_{12} & \cos k_{12} & 0 & 0 & 0 & 0 & 0 & -2\pi^2\,\bar{h}/\bar{a}^2\,k_{33}^2 \\
0 & \bar{h} & 0 & 0 & 0 & -1 & 0 & 0 & 0 & 0 & 0, \\
0 & 0 & 0 & 0 & 0 & 0 & 0 & 0 & 0 & 0 & 0 \\
0 & 0 & 0 & 0 & 0 & 0 & 0 & 0 & 0 & 0 & 0 \\
0 & 0 & 0 & \sin k_{13} & \cos k_{13} & 1 & 1 & 0 & 0 & 0 & 0 \\
0 & 0 & 0 & k_{13}\cos k_{13} & -k_{13}\sin k_{13} & 1 & 0 & 0 & 0 & 0 & 0
\end{array}
\qquad (39)
$$

may not be a useful indication of the load-carrying capacity of the delaminated plate. In some cases it may be significantly smaller than the elastic collapse load in the postbuckling regime, especially if the laminate contains a relatively long and thin delamination. In order to determine the ultimate load capacity, and the possibility of spreading of the damaged (delaminated) area to the undamaged area, the post-buckling solution is employed. Delamination growth (if it occurs) is assumed to occur in its own plane and, it is governed by the Griffith fracture criterion.

If growth takes place, it is important to examine whether the growth could be arrested at a later stage or not. The energy release rate has been used to determine whether the delamination growth is stable or unstable. The path-independent J-integral (27) has been used to obtain the energy release rate.

Also, the present model will be used to study the effect of the presence of coupling between bending and stretching on delamination growth. In this aspect, a delaminated plate in the form of unsymmetric crossply laminate is studied. Note that for such geometry there is coupling between bending and stretching regardless of the level of the applied load, and therefore the possibility of bifurcational buckling does not exist.

III.3.1 Mathematical Formulation of Delamination Growth

In deriving the equations governing the delamination growth, the case of symmetric delamination, where the delamination is located symmetrically w.r.t. the two ends of the plate, will be considered. Also, a clamped-clampled boundary condition is assumed. In the following analysis, the case of plate strip will be considered ($\varepsilon_y = 0$). The model will handle

both cases; the case for which the primary state is membrane one and the case where there is a coupling between bending and stretching.

The stress resultants and bending moments are given by (26);

$$\begin{Bmatrix} N \\ M \end{Bmatrix} = \begin{bmatrix} A & -B \\ B & -D \end{bmatrix} \begin{Bmatrix} \varepsilon^0 \\ \kappa \end{Bmatrix} \tag{40}$$

where for the plate strip

$$\begin{aligned} \{\varepsilon^0\}^T &= \{\varepsilon_x^0 \quad 0 \quad 0\} \\ \{\kappa\}^T &= \{w_{,xx} \quad 0 \quad 0\} \end{aligned} \tag{41}$$

Note that for both the orthotropic plate and cross-ply laminate

$$A_{13} = A_{23} = B_{13} = B_{23} = D_{13} = D_{23} = 0 \tag{42}$$

The equilibrium equations for plate (i) reduces to:

$$N_{xx_i} = \text{constant} = -\bar{P}_i \qquad i=1,2,3,4 \tag{43}$$

$$M_{xx_i,xx} + N_{xx_i} w_{i,xx} = 0 \qquad i=1,2,3,4 \tag{44}$$

where

$$M_{xx_i} = -\left(\frac{B_{xx}}{A_{xx}}\right)_i \bar{P}_i - \left(D_{xx} - \frac{B_{xx}^2}{A_{xx}}\right)_i w_{i,xx} \tag{45}$$

Substitution of the expression for N_{xx} and M_{xx} into the equilibrium equations, Eqs. (43,44) yields

$$W_{i,xxxx} + \frac{\bar{P}_i}{\left(D_{xx} - \frac{B_{xx}^2}{A_{xx}}\right)_i} W_{i,xx} = 0 \qquad (46)$$

To obtain the in-plane displacement we have

$$\varepsilon^0_{xx_i} = -\frac{\bar{P}_i}{A_{xx_i}} + \left(\frac{B_{xx}}{A_{xx}}\right)_i W_{i,xx}$$

$$= u^0_{i,x} + \tfrac{1}{2} W^2_{i,x} \qquad (47)$$

i.e.

$$u^0 = -\frac{\bar{P}_i}{A_{xx_i}} x + \left(\frac{B_{xx}}{A_{xx}}\right)_i W_{i,x} - \tfrac{1}{2}\int W^2_{i,x}\, dx \qquad (48)$$

For each part of the four parts (plates) of the delaminated plate the in-plane displacement and transverse displacement are given by:

$$u_i(x, z_i) = u^0_i(x) - z_i W_{i,x}$$

$$= -\frac{\bar{P}_i}{A_{xx_i}} x + \left(\frac{B_{xx_i}}{A_{xx_i}} - z_i\right) W_{i,x} - \tfrac{1}{2}\int W^2_{i,x}\, dx$$

$$i = 1, 2, 3, 4 \qquad (49)$$

$$W_i(x) = a_{i1} \sin k_i x + a_{i2} \cos k_i x + a_{i3} x + a_{i4} \qquad (50)$$

where

$$k_i^2 = \frac{\bar{P}_i}{\left(D_{xx} - \frac{B_{xx}^2}{A_{xx}}\right)_i} \qquad i = 1, 2, 3, 4 \qquad (51)$$

For symmetric delamination with clamped-damped boundary conditions, Eq. (24b) could be simplified to:

$$W_1(x) = A(\cos k_1 x - 1) \qquad 0 \le x \le \ell_1 \qquad (52a)$$

$$W_2(x) = A\left\{\cos k_1 \ell_1 - 1 + \frac{k_1 \sin k_1 \ell_1}{k_2 \sin k_2 a_2}\left[\cos k_2 \frac{a_2}{2} - \cos k_2\left(\ell_1 + \frac{a_2}{2} - x\right)\right]\right\}$$

$$\ell_1 \le x \le \ell_1 + \frac{a_2}{2} \qquad (52b)$$

$$W_3(x) = A\left\{\cos k_1 \ell_1 - 1 + \frac{k_1 \sin k_1 \ell_1}{k_3 \sin k_3 a_2}\left[\cos k_3 \frac{a_2}{2} - \cos k_3\left(\ell_1 + \frac{a_2}{2} - x\right)\right]\right\}$$

$$\ell_1 \le x \le \ell_1 + a_2 \qquad (52c)$$

The displacements U_i and W_i ($i = 1,2,3$) are now given in terms of only three unknowns A, K_2 and K_3, since K_1 is given in terms of the applied load $\bar{P}$. To determine these three unknowns, three equations are required. The required equations are the continuity in forces and moments as well as continuity in in-plane displacement.

- continuity in forces

$$\bar{P}_1 = \bar{P}_2 + \bar{P}_3 \qquad (53)$$

- continuity in moments (see Fig. 2)

$$M_1 = M_2 + M_3 - \bar{P}_2 \frac{h}{2} + \bar{P}_3 \frac{H}{2} \qquad (54)$$

Using the expressions for M_1, M_2 & M_3 gives

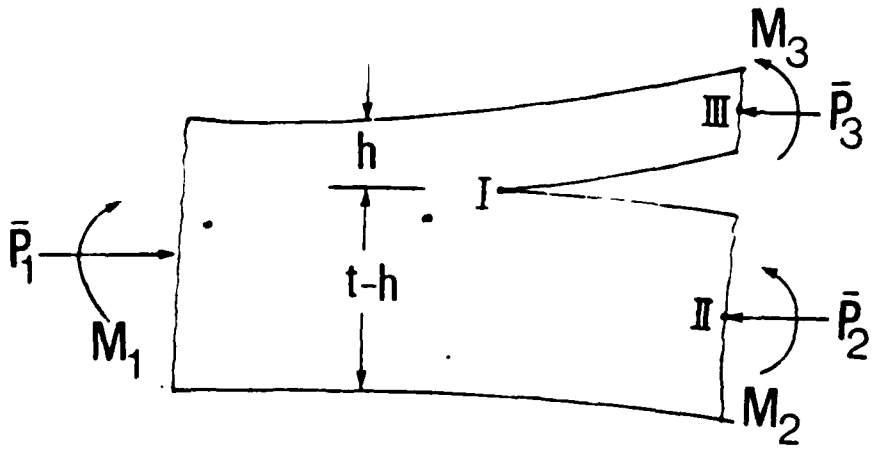

Fig. 2 Applied Moments and Forces

$$-\left(\frac{B_{xx}}{A_{xx}}\right)_1 \bar{P}_1 + \left(D_{xx} - \frac{B_{xx}^2}{A_{xx}}\right)_1 \frac{K_1}{\tan K_1 \ell_1}\,\theta = -\left(\frac{B_{xx}}{A_{xx}}\right)_2 \bar{P}_2 - \left(D_{xx} - \frac{B_{xx}^2}{A_{xx}}\right)_2 \frac{K_2}{\tan K_2 \frac{a}{2}}\,\theta$$

$$-\left(\frac{B_{xx}}{A_{xx}}\right)_3 \bar{P}_3 - \left(D_{xx} - \frac{B_{xx}^2}{A_{xx}}\right)_3 \frac{K_3}{\tan K_3 \frac{a}{2}}\,\theta - \bar{P}_2 \frac{h}{2} + \bar{P}_3 \frac{H}{2} \qquad (55)$$

where

$$\theta = A K_1 \sin K_1 \ell_1 \qquad (56)$$

- continuity in in-plane displacement (see Fig. 2)

$$u_{III} - u_I = u_{II} - u_I \qquad (57)$$

$$u_3\left(\ell_1 + \frac{a}{2}, 0\right) - u_3\left(\ell_1, \frac{h}{2}\right) = u_2\left(\ell_1 + \frac{a}{2}, 0\right) - u_2\left(\ell_1, -\frac{H}{2}\right) \qquad (58)$$

Using Eqs. (49 & 58) resuls in:

$$\left(\frac{\bar{P}_2}{A_{xx_2}} - \frac{\bar{P}_3}{A_{xx_3}}\right)\frac{a}{2} + \left(\frac{B_{xx_3}}{A_{xx_3}} - \frac{B_{xx_2}}{A_{xx_2}} - \frac{t}{2}\right)\theta$$

$$+ \left\{\frac{1}{K_3 \frac{a}{2} \tan K_3 \frac{a}{2}} - \frac{1}{\sin^2 K_3 \frac{a}{2}} - \frac{1}{K_2 \frac{a}{2} \tan K_2 \frac{a}{2}} + \frac{1}{\sin^2 K_2 \frac{a}{2}}\right\}\frac{a}{8}\theta^2 = 0 \qquad (59)$$

Using Eq. (55), we have

$$\Theta = \frac{\bar{P}_3\left(\frac{H}{2} - \frac{B_{xx_3}}{A_{xx_3}}\right) - \bar{P}_2\left(\frac{h}{2} + \frac{B_{xx_2}}{A_{xx_2}}\right) + \frac{B_{xx_1}}{A_{xx_1}}\bar{P}_1}{\left(D_{xx} - \frac{B_{xx}^2}{A_{xx}}\right)_1 \frac{K_1}{\tan k_1 l_1} + \left(D_{xx} - \frac{B_{xx}^2}{A_{xx}}\right)_2 \frac{K_2}{\tan k_2 \frac{a}{2}} + \left(D_{xx} - \frac{B_{xx}^2}{A_{xx}}\right)_3 \frac{K_3}{\tan k_3 \frac{a}{2}}} \qquad (60)$$

Solving Eqs. (53, 59, & 60) simultaneously, one can obtain the values of P_1, P_2 & P_3 in terms of the applied load P. Also, once P_1, P_2 and P_3 are known, the unknown constant A could be obtained and hence, the displacement functions are known for every level of the applied load P. Now, the postbuckling solution is known and the next step is to establish a delamination growth criterion.

II.3.2 ENERGY RELEASE RATE

In the present work, it is assumed that delamination growth (if it occurs) will take place in its own plane and is governed by the Griffith fracture criterion. It is also important to find out whether this growth is stable or unstable, in doing so, one has to calculate the energy release rate (the energy required to produce a unit of new delamination).

In order to calculate the energy release rate, the path-independent J-integral is used (27). The use of the J-integral beside being helpful in avoiding the calculation of stress singularities at the delamination tip, is useful in the cases where plasticity effects are not negligible (28).

The J-integral is defined as:

$$J = \int_\Gamma \left(\frac{1}{2}\sigma_{ij}\,\varepsilon_{ij}\,dz - \sigma_{ij}\,n_j\,\frac{\partial u_i}{\partial x}\right) ds \qquad (61)$$

where Γ is a closed contour around the crack tip.

$$J = \int \left[\tfrac{1}{2} (\sigma_x' \varepsilon_x + \sigma_y' \varepsilon_y) \, dz + \sigma_x' \varepsilon_x \, dS \right]$$

$$= \int \tfrac{1}{2} (\sigma_x' \varepsilon_x - \sigma_y' \varepsilon_y) \, dS$$

but $\varepsilon_y \equiv 0$

$$G = J = \tfrac{1}{2} \int \sigma_x' \varepsilon_x \, dS \qquad (63)$$

where G is the energy release rate

but

$$\sigma_{x_i}^{k} = Q_{xx_i}^{k} \, \varepsilon_{x_i}$$

$$= Q_{xx_i}^{k} \left\{ - \frac{\bar{P}_i}{A_{xx_i}} + \frac{B_{xx_i}}{A_{xx_i}} W_{i,xx} - \bar{z}_i W_{i,xx} \right\} \qquad (64)$$

where σ_{xi}^{k} is the stress in the x-direction in lamina number k belongs to region (i).

The stress distribution is decompassed into two subsystems, as in Refs (5,29), (a) a continuous stress field, which makes no constribution to the J-integral and (b) a subsystem (2) which does. The subsystem (2) contributions are:

Region (3) contributions

$$J_3 = \frac{1}{2} \int_{-\frac{h}{2}}^{\frac{h}{2}} Q_{xx}^{k} \left\{ \left(- \frac{\bar{P}_3}{A_{xx_3}} + \frac{B_{xx_3}}{A_{xx_1}} W_{3,xx} - \bar{z} W_{3,xx} \right) \right.$$

$$-\left[-\frac{\bar{P}_1}{A_{xx_1}}+\frac{B_{xx_1}}{A_{xx_1}}w_{1,xx}-(\eta-\frac{H}{2})w_{1,xx}\right]\Bigg\}^2 d\eta \qquad (65)$$

Note that the above integration is calculated at the cross section $x = \ell_1$.

$$J_3=\frac{1}{2}A_{xx_3}\left\{\frac{\bar{P}_1}{A_{xx_1}}-\frac{\bar{P}_3}{A_{xx_3}}+\left(\frac{B_{xx_1}}{A_{xx_1}}-\frac{B_{xx_3}}{A_{xx_3}}+\frac{H}{2}\right)\frac{K_1}{\tan K_1\ell_1}\theta\right\}^2$$

$$+\frac{1}{2}\left(D_{xx}-\frac{B_{xx}^2}{A_{xx}}\right)_3\left(\frac{K_1}{\tan K_1\ell_1}+\frac{K_3}{\tan K_3\frac{a}{2}}\right)^2\theta^2 \qquad (66)$$

Region (2) contribution

$$J_2=\frac{1}{2}A_{xx_2}\left\{\frac{\bar{P}_1}{A_{xx_1}}-\frac{\bar{P}_2}{A_{xx_2}}+\left(\frac{B_{xx_1}}{A_{xx_1}}-\frac{B_{xx_2}}{A_{xx_2}}-\frac{h}{2}\right)\frac{K_1}{\tan K_1\ell_1}\theta\right.$$

$$\left.+\frac{1}{2}\left(D_{xx}-\frac{B_{xx}^2}{A_{xx}}\right)_2\left(\frac{K_1}{\tan K_1\ell_1}+\frac{K_2}{\tan K_2\frac{a}{2}}\right)^2\theta^2\right. \qquad (67)$$

$$G=J_{total}=J_2+J_3 \qquad (68)$$

II.3.3 End Shortening and Delamination Opening

As we will see later, the knowledge of the end shorting and delamination opening will help in some cases to find the load carrying capacity of the system.

$$\Delta L = -2\left\{ U_1(l_1) - U_1(0) + U_3\left(l_1 + \frac{a}{2}\right) - U_3(l_1)\right\} \qquad (69a)$$

$$= 2\left\{ \frac{\bar{P}_1}{A_{xx_1}} l_1 + \frac{\bar{P}_3}{A_{xx_3}} \frac{a}{2} + \left(\frac{B_{xx_1}}{A_{xx_1}} - \frac{B_{xx_3}}{A_{xx_3}} + \frac{H}{2}\right)\theta \right.$$

$$\left. + \left(\frac{l_1}{\sin^2 k_1 l_1} - \frac{1}{k_1 \tan k_1 l_1} + \frac{a/2}{\sin^2 k_3 \frac{a}{2}} - \frac{1}{k_3 \tan k_3 \frac{a}{2}}\right)\frac{\theta^2}{4}\right\} \qquad (69b)$$

where ΔL is the end shortening

delamination opening $= w_3\left(l_1 + \frac{a}{2}\right) - w_2\left(l_1 + \frac{a}{2}\right)$ (70a)

$$\Delta w = \left[\frac{1}{k_3 \tan k_3 \frac{a}{2}} - \frac{1}{k_3 \sin k_3 \frac{a}{2}} - \frac{1}{k_2 \tan k_2 \frac{a}{2}}\right.$$

$$\left. + \frac{1}{k_2 \sin k_2 \frac{a}{2}}\right]\theta \qquad (70b)$$

First the following non-dimensional parameters are introduced.

$$\bar{A}_{xx_i} = \frac{A_{xx_i}}{Q_{xx} t} \quad ; \quad \bar{B}_{xx_i} = \frac{B_{xx_i}}{Q_{xx} t^2} \quad ; \quad \bar{D}_{xx_i} = \frac{D_{xx_i}}{Q_{xx} t^3}$$

$$\tilde{B}_{xx_i} = \frac{\bar{B}_{xx_i}}{\bar{A}_{xx_i}} \quad ; \quad \tilde{D}_{xx_i} = \bar{D}_{xx_i} - \frac{\bar{B}^2_{xx_i}}{\bar{A}_{xx_i}} \quad ; \quad DC_{xx_i} = \frac{\tilde{D}_{xx_i}}{\bar{A}_{xx_i}} \qquad (71)$$

$$D_{xx_{eff_i}} = D_{xx_i} - \frac{B_{xx_i}^2}{A_{xx_i}}$$

$$\bar{P}_1 = \frac{\bar{P}_1}{\frac{4\pi^2 D_{xx_{1\,eff}}}{L^2}} \quad ; \quad \bar{P}_3 = \frac{\bar{P}_3}{\frac{4\pi^2 D_{xx_{3\,eff}}}{a^2}} \qquad (72)$$

$$\bar{K}_1 = K_1 L = 2\pi\sqrt{\bar{P}_1}$$

$$\bar{K}_3 = K_3 \frac{a}{2} = \pi\sqrt{\bar{P}_3} \qquad (73)$$

$$\bar{K}_2 = K_2 \frac{a}{2} = \sqrt{\left[\left(\frac{\bar{a}}{2}\bar{k}_1\right)^2 - \frac{\tilde{D}_{xx_3}}{\tilde{D}_{xx_1}}\bar{K}_3^2\right]\frac{\tilde{D}_{xx_1}}{\tilde{D}_{xx_2}}}$$

$$\bar{\theta} = \theta\,\frac{L}{t}$$

$$\bar{\Delta L} = (\Delta L)\frac{L}{t^2} \quad ; \quad \Delta w = \frac{\Delta w}{t} \quad ; \quad \bar{G}_1 = G\,\frac{L^4}{t^5} \qquad (74)$$

In terms of the above nondimensional parameters, the equations governing the behavior, Eqs (53, 59, & 60) and growth Eq. (68) of the delaminated plate can be summarized as:

$$\left(\frac{2}{\bar{a}}\right)^2\left\{\bar{K}_2^2 DC_{xx_2} - \bar{K}_3^2 DC_{xx_3}\right\} + \left(\frac{2}{\bar{a}}\right)\left\{\tilde{B}_{xx_3} - \tilde{B}_{xx_2} - .5\right)\bar{\theta}$$

$$+\frac{1}{4}\bar{\theta}^2\left[\frac{1}{\sin^2\bar{K}_2} - \frac{1}{\bar{K}_2\tan\bar{K}_2} - \frac{1}{\sin^2\bar{K}_3} + \frac{1}{\bar{K}_3\tan\bar{K}_3}\right] = 0 \qquad (75)$$

where

$$\bar{\theta} = \frac{\bar{K}_1^2\left(\tilde{B}_{xx_1} - \tilde{B}_{xx_2} - .5\bar{h}\right) - \bar{K}_3\left(\frac{2}{\bar{a}}\right)^2 \frac{\tilde{D}_{xx_3}}{\tilde{D}_{xx_1}}\left(\tilde{B}_{xx_3} - \tilde{B}_{xx_2} - .5\right)}{\frac{\bar{K}_1}{\tan\bar{K}_1\bar{\ell}_1} + \frac{2}{\bar{a}}\left[\frac{\bar{K}_2}{\tan\bar{K}_2}\frac{\tilde{D}_{xy_2}}{\tilde{D}_{xx_1}} + \frac{\bar{K}_3}{\tan\bar{K}_3}\frac{\tilde{D}_{xy_3}}{\tilde{D}_{xy_1}}\right]} \tag{76}$$

$$K_2 = \sqrt{\left[\left(\frac{\bar{a}}{2}\bar{K}_1\right)^2 - \frac{\tilde{D}_{xx_3}}{\tilde{D}_{xx_1}}\bar{K}_3^2\right]\frac{\tilde{D}_{xx_1}}{\tilde{D}_{xx_2}}} \tag{77}$$

$$\overline{\Delta L} = 2\left\{\bar{K}_1^2\bar{\ell}_1 DC_{xx_1} + \bar{K}_3^2\left(\frac{2}{\bar{a}}\right)DC_{xx_3} + \left(\tilde{B}_{xx_1} - \tilde{B}_{yx_3} + \frac{\bar{H}}{2}\right)\bar{\theta} + \frac{1}{4}\bar{\theta}^2\left[\frac{\bar{\ell}_1}{\sin^2\bar{K}_1\bar{\ell}_1} - \frac{1}{\bar{K}_1\tan\bar{K}_1\bar{\ell}_1} + \frac{\bar{a}_2}{\sin^2\bar{K}_3} - \frac{\bar{a}_2}{\bar{K}_3\tan\bar{K}_3}\right]\right\} \tag{78}$$

$$\overline{\Delta W} = \bar{\theta}\left[\frac{\frac{\bar{a}}{2}}{\bar{K}_3\tan\bar{K}_3} - \frac{\bar{a}_2}{\bar{K}_3\sin\bar{K}_3} - \frac{\bar{a}_2}{\bar{K}_2\tan\bar{K}_2} + \frac{\frac{\bar{a}}{2}}{\bar{K}_2\sin\bar{K}_2}\right] \tag{79}$$

$$\bar{G} = \frac{1}{2}\bar{A}_{xx_2}\left[\bar{K}_1^2 DC_{xx_1} - \left(\frac{2}{\bar{a}}\right)^2\bar{K}_2^2 DC_{xx_2} + \left(\tilde{B}_{xx_1} - \tilde{B}_{xx_2} - .5\bar{h}\right)\frac{\bar{K}_1}{\tan\bar{K}_1\bar{\ell}_1}\bar{\theta}\right]^2$$

$$+ \frac{1}{2}\tilde{D}_{xx_2}\left(\frac{\bar{K}_1}{\tan\bar{K}_1\bar{\ell}_1} + \frac{2}{\bar{a}}\frac{\bar{K}_2}{\tan\bar{K}_2}\right)^2\bar{\theta}^2$$

$$+ \frac{1}{2}\bar{A}_{xx_3}\left[\bar{K}_1^2 DC_{xx_1} - \left(\frac{2}{\bar{a}}\right)^2\bar{K}_3^2 DC_{xx_3} + \left(\tilde{B}_{xx_1} - \tilde{B}_{xx_3} + .5\bar{H}\right)\frac{\bar{K}_1}{\tan\bar{K}_1\bar{\ell}_1}\bar{\theta}\right]^2$$

$$+\frac{1}{2}\tilde{D}_{xx_3}\left(\frac{\bar{k}_1}{\tan\bar{k}_1\bar{\ell}_1}+\frac{2}{\bar{a}}\frac{\bar{k}_2}{\tan\bar{k}_2}\right)^2\bar{\theta}^2 \qquad (80)$$

These three equations, Eqs. (78)-(80) are valid for any plate with across the width (one-dimensional) delamination, provided that the assumption of cylindrical bending deformation holds ($\varepsilon_y \equiv 0$).

III RESULTS AND DISCUSSION

The Georgia Tech high speed digital computer CDC-Cyber 70, Model 74-28 was employed for generating results. These results are presented both in tabular and graphical form.

III.1 Buckling Results

III.1.1 Orthotropic Plate

Results for buckling loads of a delaminated orthotropic plate are generated.

Table 1 shows values of critical loads, $\bar{p}$, of a clamped configuration with a symmetric delamination [see Eq. (30)], for several values of the delamination length parameter, $\bar{a}$, and of the delamination thickness parameter, $\bar{h}$.

The last row gives the sum of the buckling loads of the two parts, if the delamination extends through the entire length $\bar{a} = 1$. This sum, $\bar{p}$, is a measure of the load carrying capacity of the completely damaged configuration

$$\bar{P}_{dam} = \bar{h}^3 + (1-\bar{h})^3 \qquad (81)$$

These results are also shown graphically in Fig. 3. It is clearly seen from these results, that as long as $\bar{a} \leq \bar{h}$, buckling load is not affected appreciably by the presence of the delamination provided that the delamination thickness is relatively small ($\bar{h} < .2$). For the same condition of $\bar{a} \leq \bar{h}$, the presence of the delamination becomes more pronounced as one approaches a midthickness delamination ($\bar{h} = .5$). Note that for this extreme case, when $\bar{a} = \bar{h} = .5$, $\bar{P}_{cr} = .69$ and $\bar{P}_{cr}$ increases as $\bar{a}$ becomes smaller and smaller. On the other hand, when $\bar{a} > \bar{h}$ the buckling load is

Table 1. Buckling Loads for a Symmetric Delamination-Clamped Boundaries

$\bar{a}$ \ $\bar{h}$	.02	.05	.10	.20	.30	.40	.50
.025	.6399889	.9999989	.9999996	.9999999	.9999999	.9999999	.9999999
.05	.1599975	.9949313	.9999824	.9999929	.9999949	.9999958	.9999960
.10	.0399994	.2499388	.9799200	.9997142	.9998254	.9998600	.9998683
.15	.0177775	.1110863	.4434620	.9965731	.9985213	.9988911	.9989777
.20	.0099999	.0624871	.2495341	.9264435	.9923920	.9950435	.9955576
.25	.0063999	.0399923	.1597332	.6255729	.9661928	.9835314	.9859276
.30	.0044444	.0277728	.1109427	.4371092	.8582246	.9543270	.9638297
.40	.0025000	.0152263	.0624213	.2470476	.5313834	.7883037	.8480737
.50	.0016000	.0099987	.0399587	.1585467	.3469048	.5675410	.6895626
.60	.0011111	.0069437	.0277551	.1103405	.2435310	.4123884	.5411401
.70	.0008163	.0051017	.0203958	.0812210	.1803553	.3111042	.4309655
.80	.0006250	.0039061	.0156187	.0622944	.1390114	.2428107	.3514201
.90	.0004938	.0030863	.0123432	.0493028	.1104955	.1948719	.2923016
1.00	.0004000	.0025000	.0100000	.0400000	.0900000	.1600000	.2500000
$\bar{r}_{dam}$	.9412000	.8572000	.7300000	.5200000	.3700000	.2800000	.2500000

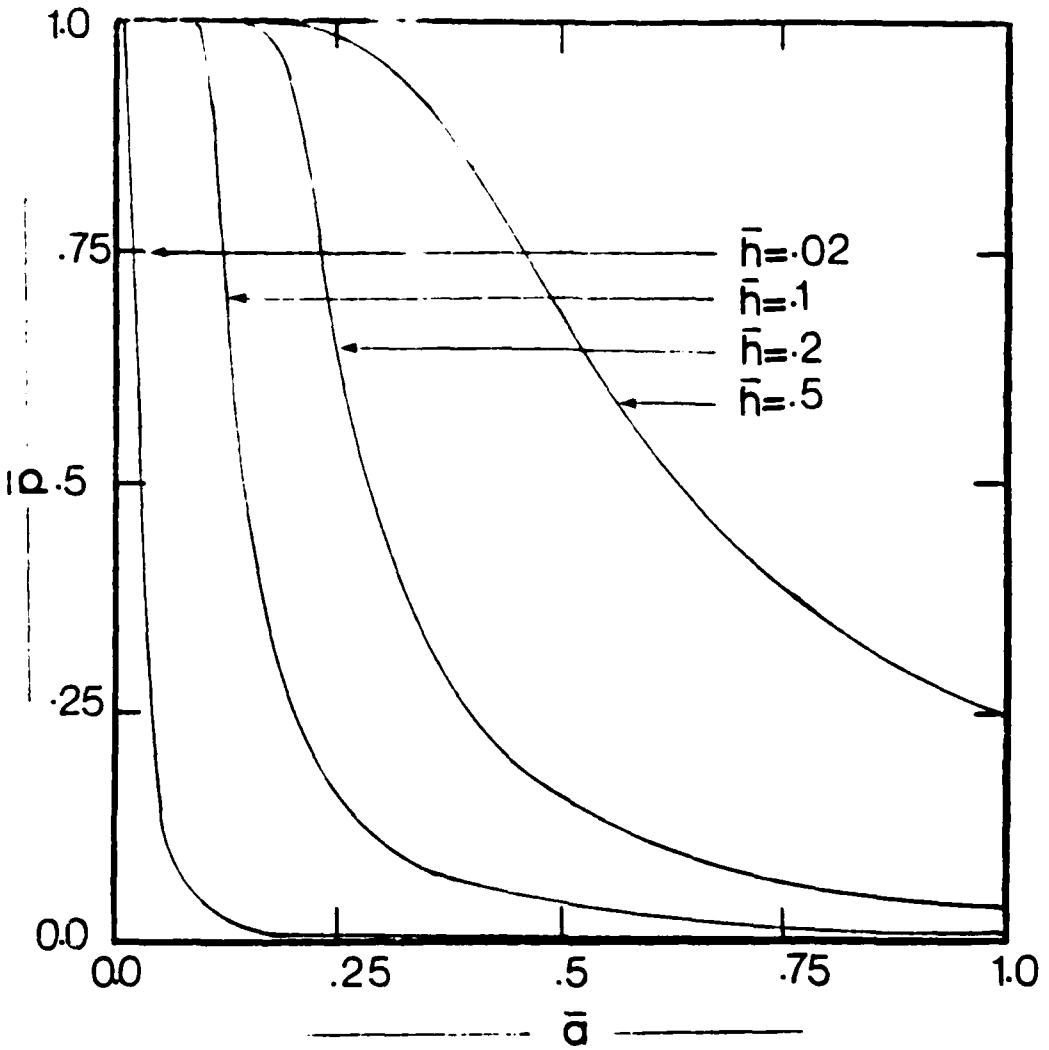

Fig. 3 Effect of Symmetric Delamination on Buckling Loads of Wide Column with Clamped Ends

greatly affected and it drops drastically, especially for the smaller values of the delamination thickness.

A comparison of the buckling loads with the buckling load for the completely damaged system (last number in each column) reveals certain observations which suggest related conclusions. When $\bar{a} \leq \bar{h}$ the values for $\bar{P}_{cr}$ are higher than $\bar{P}_{dam}$. This suggest that for these geometries the load carrying capacity of the system is related to and measured by the buckling load of the delaminated configuration. On the other hand, for $\bar{a} > \bar{h}$ buckling occurs at low values of the applied load. Then if the load is further increased this may lead to delamination growth and the damaged area may extend along the enire length of the system. This of course depends on the fracture toughness of the material, but the implication is that $\bar{P}_{dam}$ is a good lower bound for the load carrying capacity of the delaminated configuration. The problem of postbuckling behavior, delamination growth and accurate estimation of the load carrying capacity of a delaminated configuration is the subject of Part III.2 of this report.

On Table 2, the value of the load in region 3 at the instant of buckling is given for the same range of parameters, $\bar{a}$ and $\bar{h}$, as on Table 1. These results are also for the case of clamped supports. The values for this region 3 load are nondimensionalized with respect to the critical load of the region 3 geometry, as if its ends were clamped. This is done primarily for finding the range of parameters $\bar{a}$ and $\bar{h}$ for which thin film analysis holds [2]. Clearly, when $\bar{p}_3$ is close to unity, thin film analysis is applicable and thus delamination growth can be treated by the simpler analysis [2] developed for the case of thin film behavior. Thin film behavior implies that region 3 only experiences buckling and postbuckling deformations while the remaining of the plate remains undeformed. For

Table 2. Region of Applicability of Thin Film Analysis for a Symmetric Delaminated, Wide Column with Clamped Ends

$\bar{a}$ \ $\bar{h}$	.02	.05	.10	.20	.30	.40	.50
.025	.9999827	.2499997	.0625000	.0156250	.0069444	.0039062	.0025000
.05	.9999845	.9949313	.2499956	.0625000	.0277776	.0156249	.0100000
.10	.9999855	.9997555	.9799200	.2499286	.1110917	.0624912	.0399947
.15	.9999863	.9997769	.9977894	.5605725	. 496303	.1404691	.0899080
.20	.9999871	.9997932	.9981364	.9264439	.4410631	.2487609	.1592892
.25	.9999881	.9998079	.9983327	.9774573	.6709672	.3841920	.2464812
.30	.9999889	.9998216	.9984847	.9834956	.8582246	.5368090	.3469787
.40	.9999905	.9998483	.9987409	.9881904	.9446817	.7883037	.5427671
.50	.9999923	.9998741	.9989685	.9909166	.9636244	.8867828	.6895626
.60	.9999937	.9998995	.9991833	.9930647	.9741242	.9278740	.7792417
.70	.9999953	.9999261	.9993921	.9949577	.9819344	.9527566	.8446920
.80	.9999970	.9999503	.9995985	.9967103	.9885257	.9712427	.8996356
.90	.9999985	.9999750	.9997994	.9983807	.9944594	.9865390	.9502971
1.00	1.000000	1.000000	1.000000	1.000000	1.000000	1.000000	1.000000

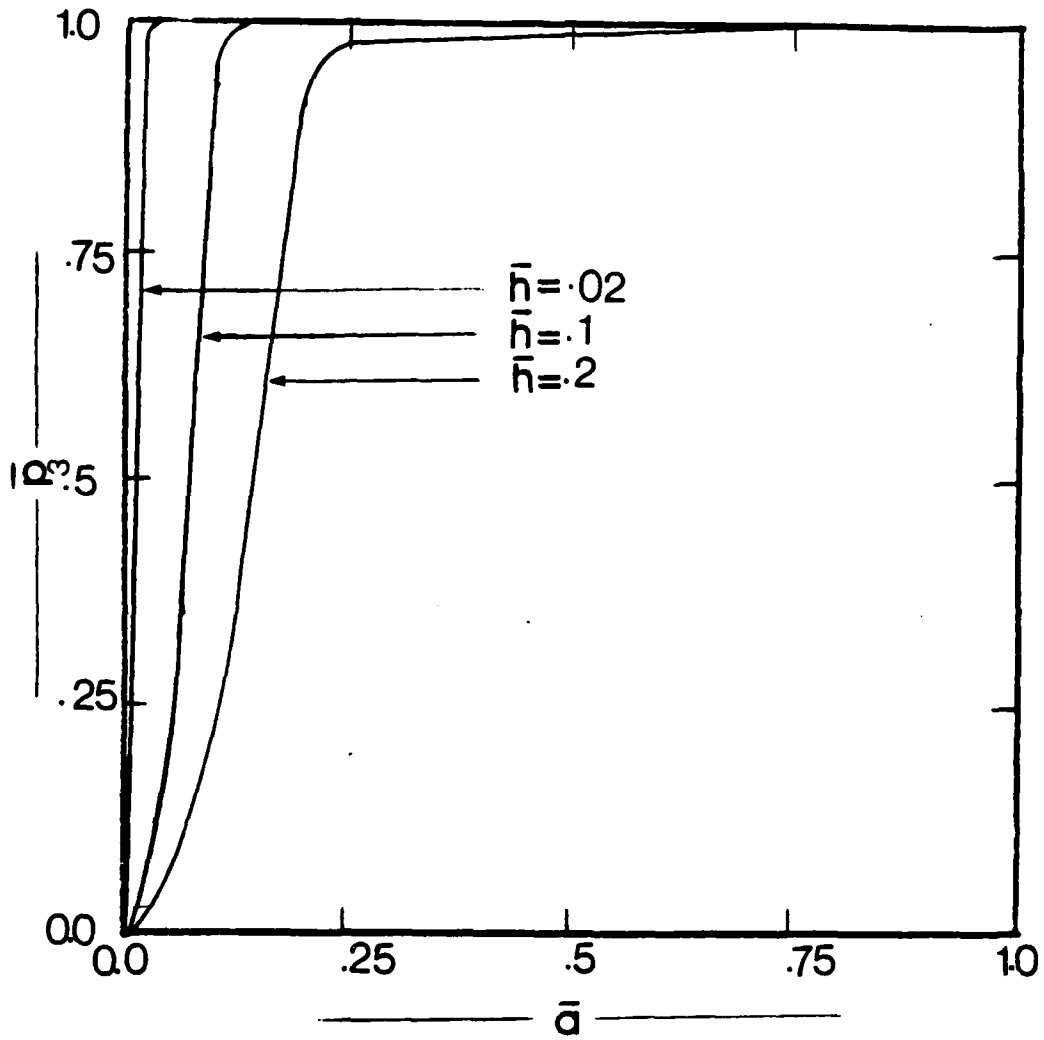

Fig. 4 Region of Applicability of Thin Film Analysis for a Symmetric Delaminated. Wide Column with Clamped Ends

small values of $\bar{h}$, say $\bar{h} = 0.02$, thin film is applicable for all values of $\bar{a}$. As $\bar{h}$ increases, towards its maximum value of 0.5, the region of applicability of thin film analysis is confined towards the high $\bar{a}$-value region. The results of Table 2 are presented graphically on Fig. 4.

Similary results are presented on Tables 3 and 4 and Figures 5 and 6 respectively for the case of simply supported ends. On Table 3, $\bar{p}$ is nondimensinalized with respect to the perfect geometry critical load for simply supported ends. The values corresponding of $\bar{p}_{dam}$ (last row), are the sum of the contributions of both parts acting independent of each other and both being simply supported. This may be questionable, because a better description of the completely damaged plate is needed. For example, if, when the delamination extends along the entire length, the thin part is lost (it becomes disconnected) then a better measure for $\bar{p}_{dam}$ would be $(1-\bar{h})^3$ rather than $\bar{h}^3 + (1-\bar{h})^3$. It is also worth mentinoing here that the values ($\bar{P}$) corresponding to $\bar{a} = 1$ (next to the last row) are calculated under the assumption that both parts (regions 3 and 2) have the same slope at the boundaries.

The trends, observed in the case of clamped supports, are also observed here but the regions seem to have shifted. For instance, on Table 1 it was observed that, as long as $\bar{a} \leq \bar{h}$, the buckling load was not affected appreciably by the presence of the delamination, for relatively small delamination thicknesses. Here on Table 3 this statement is also true but $a \leq h$ must be replaced by $\bar{a} \leq 2\bar{h}$, and so on.

So far results have been presented and discussed for the case of symmetrically located delaminations [$\bar{\ell}_1 = 0.5(1-a)$].

Next, results are presented on Tables 5, 6, 7 and 8 for the case for which the delamination is asymmetrically located.

Table 3. Buckling Loads for a Symmetric Delamination Simply Supported Boundaries

$\frac{a}{h}$	.02	.05	.10	.20	.30	.40	.50
.025	.9999999	.9999999	1.000000	1.000000	1.000000	1.000000	1.000000
.05	.9999978	.9999978	.9999992	.9999996	.9999997	.9999999	.9999999
.10	.1599973	.9929014	.9999653	.9999851	.9999897	.9999914	.9999919
.15	.0711099	.4443054	.9995550	.9998786	.9999198	.9999342	.9999379
.20	.0399994	.2499288	.9722769	.9994269	.9996506	.9997188	.9997368
.25	.0255996	.1599562	.6376329	.9979332	.9988852	.9991293	.9991891
.30	.0177775	.1110815	.4431942	.9932354	.9970554	.9977368	.9979614
.40	.0099996	.0624836	.2493840	.9016443	.9851533	.9902270	.9912249
.50	.0064000	.0399897	.1596320	.6177589	.9402233	.9686038	.9729376
.60	.0044444	.0277707	.1108654	.4330717	.8149228	.9198068	.9343196
.70	.0032653	.0204030	.0814568	.3193488	.6484304	.8350811	.8703371
.80	.0025000	.0156210	.0623679	.2449950	.5117912	.7263620	.7867299
.90	.0019753	.0123426	.0492799	.1938276	.4105782	.6176623	.6966477
1.00	.0016000	.0099975	.0399176	.1571446	.3356235	.5228832	.6109859
$\bar{P}_{cr}$	.9412000	.8572000	.7300000	.5200000	.3700000	.2800000	.2500000

Table 4 Region of Applicability of Thin Film Analysis for a Symmetric Delaminated. Wide Column with Simply Supported Ends

$\frac{\bar{h}}{\bar{a}}$	.02	.05	.10	.20	.30	.40	.50
.025	.3906251	.0625000	.0156250	.0039063	.0017361	.0009766	.0006250
.05	.9999810	.2499995	.0625000	.0156250	.0069444	.0039062	.0025000
.10	.9999834	.9929014	.2499913	.0624991	.0277775	.0156249	.0099999
.15	.9999836	.9996871	.5622497	.1406079	.0629500	.0351539	.0224986
.20	.9999838	.9997154	.9722769	.2498572	.1110723	.0624824	.0399895
.25	.9999839	.9997260	.9963014	.3898177	.1734176	.0975712	.0624493
.30	.9999840	.9997337	.9970970	.5586949	.2492638	.1403147	.0898165
.40	.9999841	.9997383	.9975360	.9016460	.4378460	.2475568	.1585960
.50	.9999842	.9997416	.9977000	.9652483	.6529328	.3783609	.2432344
.60	.9999843	.9997439	.9977883	.9744113	.6149228	.5173914	.3363550
.70	.9999843	.9997459	.9978456	.9780056	.8825858	.6393590	.4264652
.80	.9999843	.9997466	.9978860	.9799799	.9098510	.7263620	.5035072
.90	.9999843	.9997483	.9979178	.9812521	.9238010	.7817289	.5642846
1.00	.9999843	.9997483	.9979401	.9821539	.9322875	.8170050	.6109859

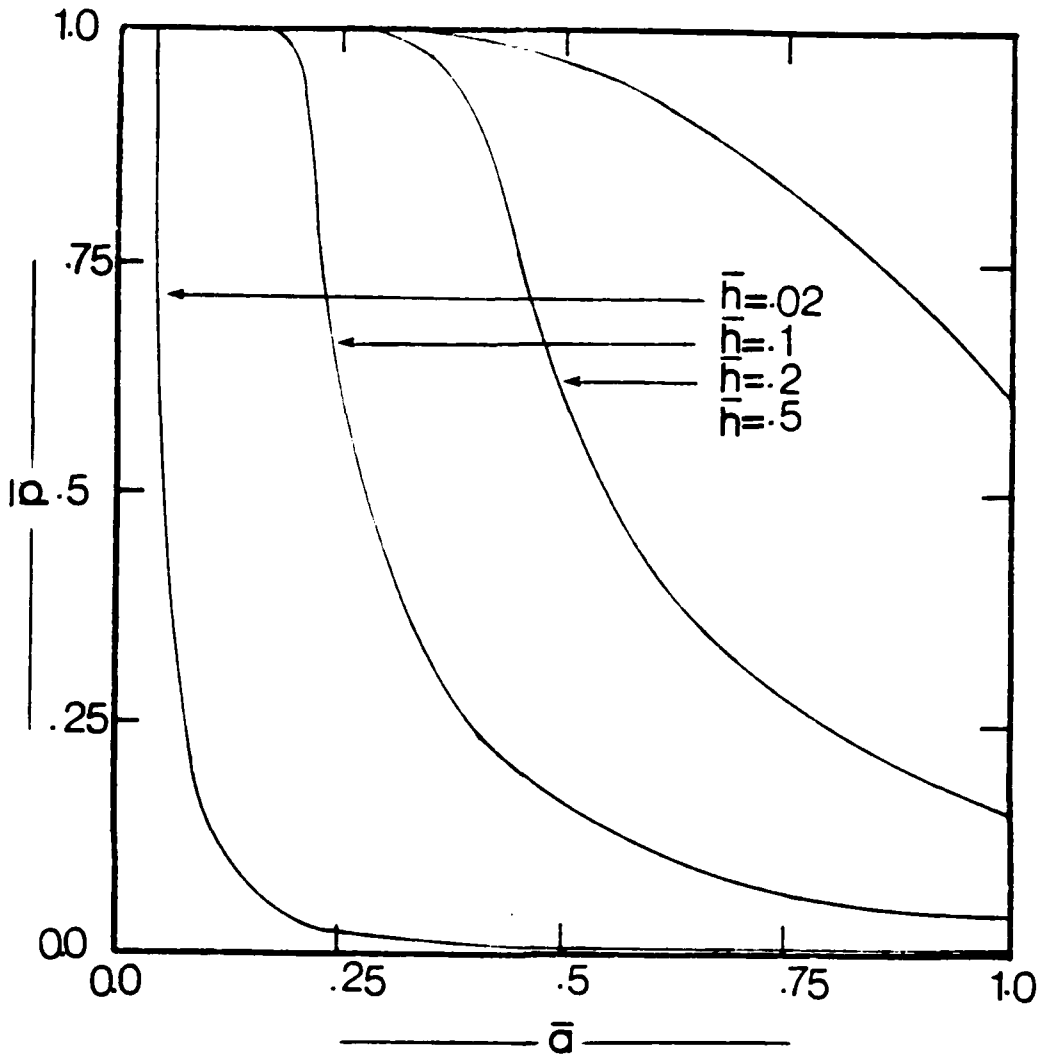

Fig. 5 Effect of Symmetric Delamination on Buckling Loads of Wide Column with Simply Supported Ends.

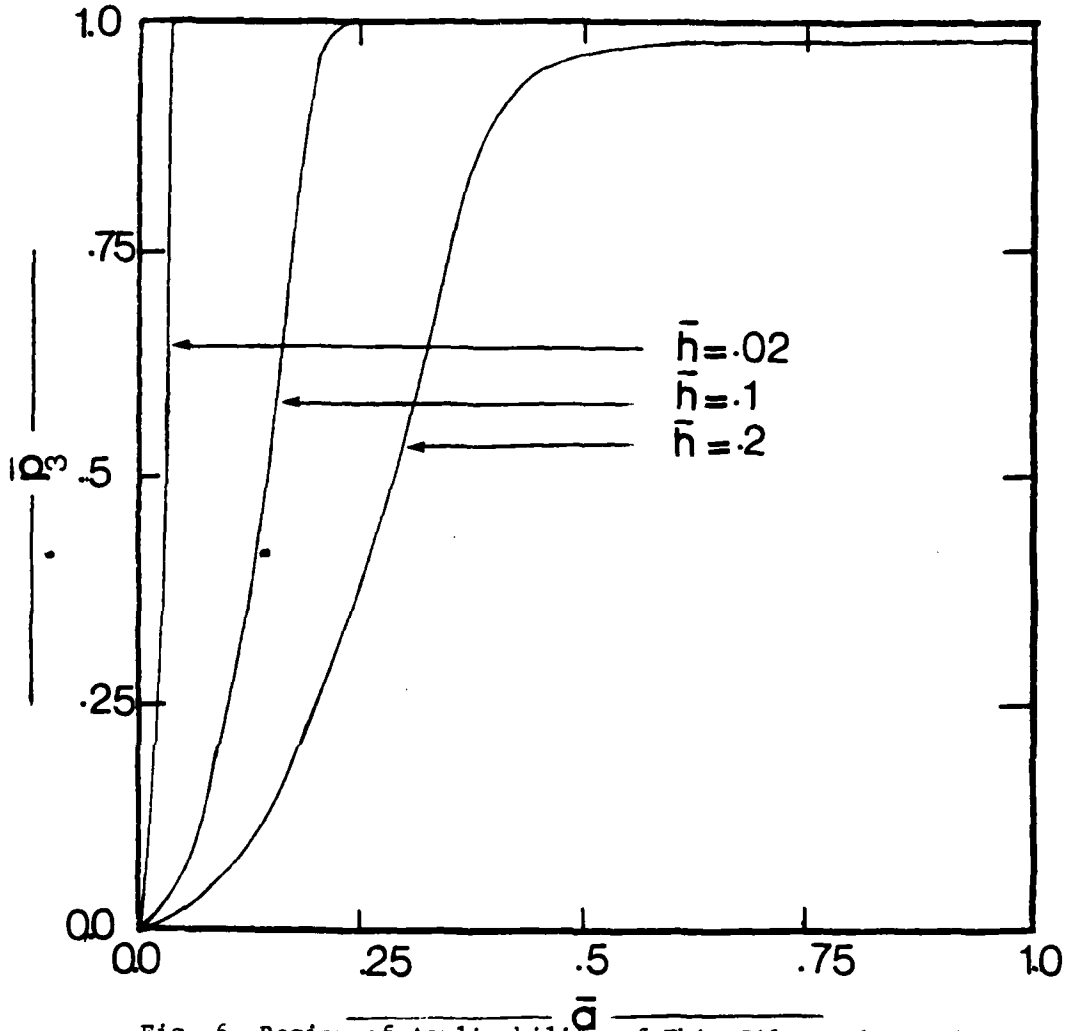

Fig. 6 Region of Applicability of Thin Film Analysis for Symmetric Delamination. Wide Column with Simply Supported Ends.

Table 5. Effect of Delamination Location on the Buckling Load (Clamped Supports; $\bar{a}$ = .1)

ℓ_1 \ $\bar{h}$	.05	.1	.2	.3	.4	.5
.0	.2499536	.9808663	.9991479	.9987055	.9980807	.9977440
.1	.2499509	.9870979	.9958626	.9922549	.9879301	.9856805
.2	.2499463	.9775824	.9938938	.9884996	.9822217	.9790165
.3	.2499418	.9668065	.9958984	.9923842	.9862422	.9861157
.45	.2499388	.9799200	.9997142	.9998254	.9998600	.9998683

Table 6. Effect of Delamination Location on the Buckling Load (Clamped Supports; $\bar{a}$ = .2)

ℓ_1 \ $\bar{h}$	.05	.1	.2	.3	.4	.5
.0	.0624932	.2497486	.9327570	.9557411	.9247731	.9051069
.1	.0624907	.2496894	.9479818	.9142127	.8652345	.8403072
.2	.0624868	.2496161	.9455077	.9194764	.8767561	.8554676
.3	.0624876	.2495566	.9309424	.9613436	.9401638	.9277638
.4	.0624871	.2495341	.9264435	.9923920	.9950435	.9955576

Table 7. Effect of Delamination Location on the Buckling Load

(Simply Supports; $\bar{a}$ = .1)

$\bar{t}_1$ / $\bar{h}$	.0	.1	.2	.3	.45
.05	.998639	.996576	.994855	.993624	.992901
.10	.999407	.999511	.999679	.999847	.999965
.20	.998517	.998790	.999232	.999674	.999985
.30	.997760	.997760	.998583	.999409	.999990
.40	.995823	.996598	.997849	.999106	.999991
.50	.995113	.996020	.997483	.998954	.999992

Table 8. Effect of Delamination Location on the Buckling Load

(Simply Supports; $\bar{a}$ = .2)

$\bar{t}_1$ / $\bar{h}$	.0	.1	.2	.3	.4
.05	.249936	.269933	.269931	.249929	.249929
.10	.988205	.981420	.976383	.973308	.972277
.20	.989043	.991885	.995416	.998312	.999429
.30	.979666	.985074	.991836	.997459	.999651
.40	.969003	.977209	.987545	.996274	.999719
.50	.963667	.973241	.985342	.995645	.999737

Tables 5 and 6 present results for the case of clamped supports, in terms of buckling loads $\bar{p}$ for various values of $\bar{h}$, and $\bar{\ell}_1$. The results on Table 5 correspond to $\bar{a} = 0.1$ and those on Table 6, to $\bar{a} = 0.2$. It is seen from Table 5 and 6 that, as long as $\bar{h} \leq \bar{a}$, the buckling load is the smallest, when the delamination is located symmetrically, with respect to the midpoint of the wide column. On the other hand, when $\bar{h} > \bar{a}$ the buckling load is the smallest when the delamination is locatd in such a way that it spans the quarter point of the wide column.

For the case of simply supported columns the results of Tables 7 and 8 reveal similar trends. For $\bar{h} < \bar{a}$, the buckling load is the smallest when the delamination is located symmetrically with respect to the midpoint of the wide column. Finally, for $\bar{h} \geq \bar{a}$, the buckling load is the smallest, when the delamination starts from the end of the wide column.

Note that in some cases, for $\bar{h} > \bar{a} = 0.2$ and clamped boundary conditions, effect of delamination on the buckling load is considerable. From Table 6 one observes that for $\bar{h} = 0.5$ $\bar{p}_{min} = 0.841$ ($\bar{\ell}_1 = 0.1$) while $\bar{p}_{max} = 0.996$ ($\bar{\ell}_1 = 0.4$).

III.1.3 Symmetric Cross-ply Plates

Results for buckling loads of delaminated plates made up of Graphite/Epoxy have been obtained.

The orthotropic axes are alternately oriented at angles 0° and 90° with the structural axes.

The elastic constants typical of this material are:

where, $E_L/E_T = 40$, $G_{LT}/E_T = .5$, $\nu_{LT} = .25$

E_L is the tensile modulus in the filament direction (30 x 10^6 psi)

E_T is the modulus in the transverse direction (.75 x 10^6 psi)

Table 9. Buckling Loads for Symmetric Cross-Ply Laminates, $[0^\circ/90^\circ/0^\circ]_{10T}$, with Clamped Ends

$\bar{a}$ \ $\bar{h}$	.1	.2	.3	.4	.5
0.05	.9999686	.9999933	.9999951	.9999958	.9999960
0.10	.9990517	.9997470	.9998327	.9998625	.9998705
0.15	.6294934	.9971932	.9985950	.9989176	.9989960
0.20	.3544494	.9605042	.9926885	.9951751	.9956418
0.25	.2269353	.6856117	.9695678	.9840387	.9862131
0.30	.1576354	.4804679	.8756095	.9560119	.9646097
0.40	.0887059	.2718917	.5517876	.7965493	.8556681
0.50	.0567913	.1745731	.3610403	.5774029	.6943155
0.60	.0394509	.1215207	.2536700	.4205562	.5460455
0.70	.0289931	.0894789	.1879582	.3176146	.4354499
0.80	.0222044	.0686417	.1449236	.2480524	.3554099
0.90	.0175493	.0543362	.1152281	.1991666	.2968545
1.00	.0142190	.0440911	.0938781	.1635797	.2531960

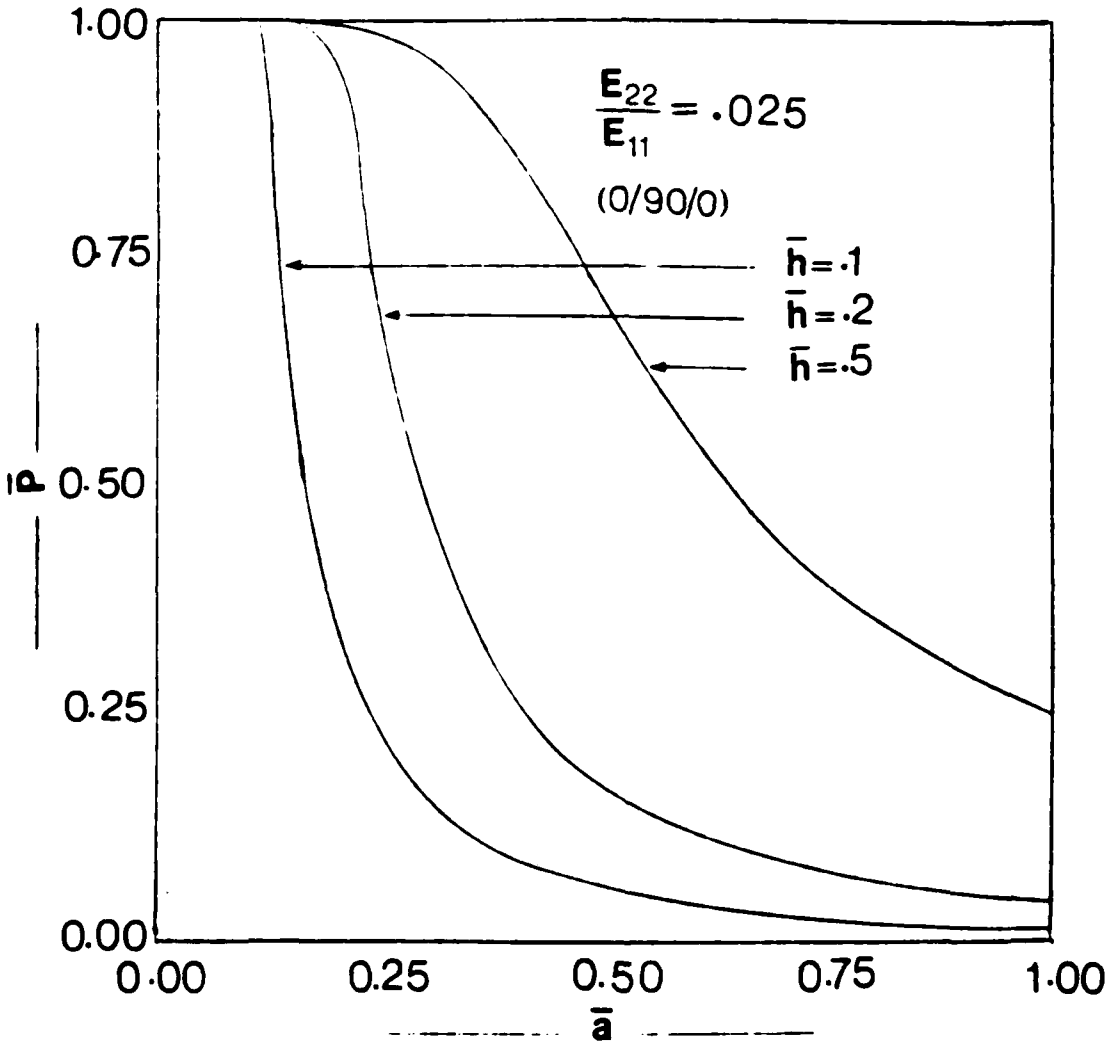

Fig. 7 Effect of Symmetric Delamination on Buckling Loads of Cross-Ply Laminates with Clamped Ends.

Table 10. Buckling Loads for Symmetric Cross-ply Laminates, $[0^\circ/90^\circ_2/0^\circ]_{10T}$, with Clamped Ends

$\frac{h}{a}$	.1	.2	.3	.4	.5
0.05	.9999907	.9999937	.9999953	.9999960	.9999961
0.10	.9994218	.9997648	.9998374	.9998647	.9998721
0.15	.7516396	.9974912	.9986399	.9989348	.9990081
0.20	.4237520	.9714079	.9931818	.9952590	.9956966
0.25	.2713595	.7242170	.9714534	.9843584	.9863974
0.30	.1885120	.5089376	.8856250	.9570613	.9651120
0.40	.1060935	.2882870	.5650983	.8017537	.8606837
0.50	.0679288	.1851633	.3703492	.5838284	.6974178
0.60	.0471911	.1289302	.2603643	.4259284	.5492680
0.70	.0346837	.0949420	.1929842	.3219117	.4384057
0.80	.0265641	.0728424	.1488349	.2515180	.3580450
0.90	.0209962	.0576684	.1183607	.2020089	.2992045
1.00	.0170128	.0468003	.0964461	.1659502	.2553130

Table 11. Buckling Loads for Symmetric Cross-ply Laminates, $[0^\circ/90^\circ_4/0^\circ]_{10T}$, with Clamped Ends

$\bar{h}$ / $\bar{a}$	.1	.2	.3	.4	.5
0.05	.9999923	.9999940	.9999953	.9999959	.9999961
0.10	.9995946	.9997816	.9998421	.9998666	.9998736
0.15	.8830985	.9977533	.9986859	.9989527	.9990209
0.20	.5003633	.9784464	.9934780	.9953480	.9957556
0.25	.3205248	.7654852	.9732843	.9846975	.9865968
0.30	.2226972	.5402340	.8954534	.9581666	.9656552
0.40	.1253515	.3064068	.5796544	.8072930	.8631029
0.50	.0802672	.1968816	.3806192	.5908523	.7008153
0.60	.0557673	.1371230	.2677667	.4318495	.5528164
0.70	.0409899	.1009933	.1985476	.3266621	.4416697
0.80	.0313961	.0774970	.1531672	.2553549	.3609600
0.90	.0248171	.0613616	.1218322	.2051583	.3018072
1.00	.0201110	.0498036	.0992930	.1685782	.2576600

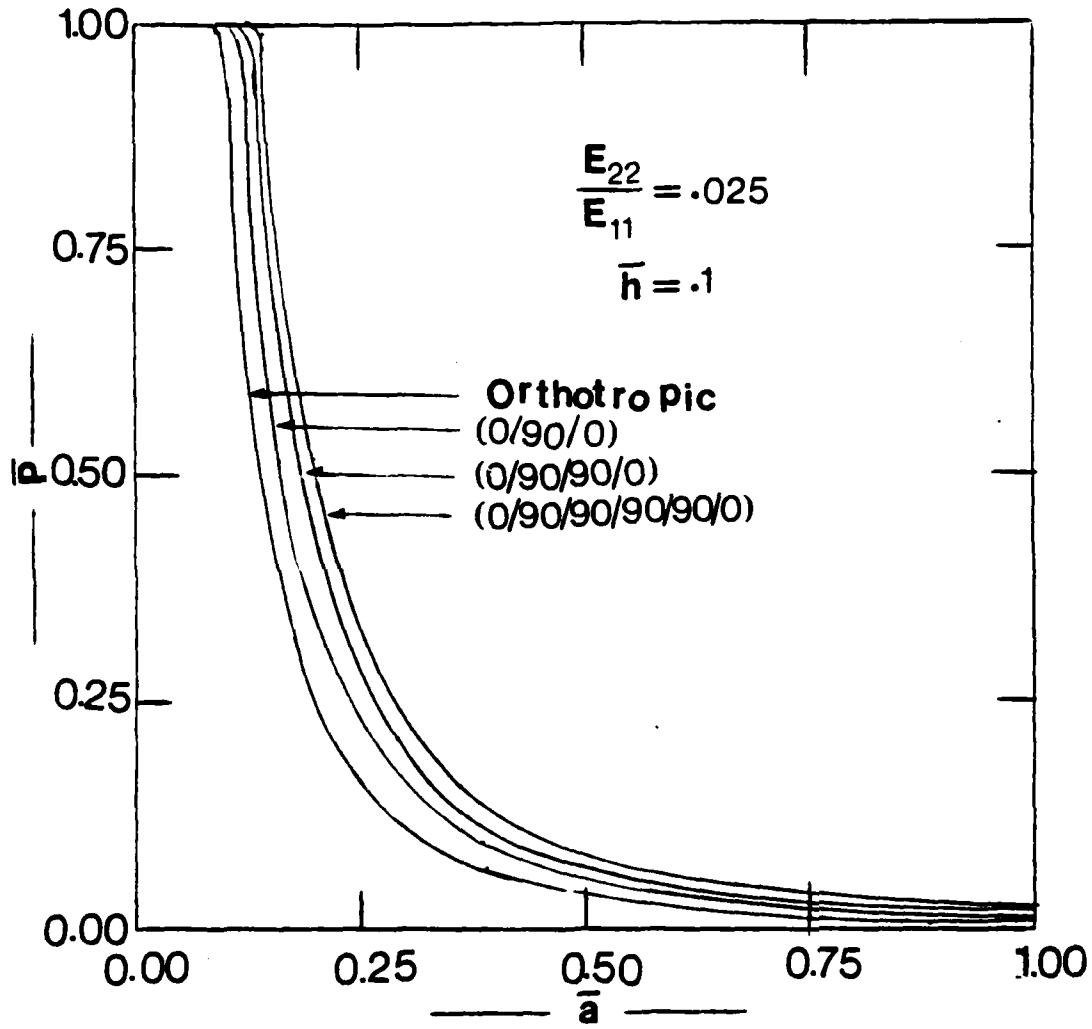

Fig. 8 Effect of Stacking Sequence on Buckling Loads of Delaminated Plate

G_{LT} is the shear modulus (.375 x 10_6 psi)

ν_{L_T} is Poisson's ratio

Results are generated for laminates with the stacking sequences, $[0^o/90^o/0^o]_{10T}$, $[0^o/90^o_2/0^o]_{10T}$. The effect of delamination length and thickness on those buckling loads is studied. Note that $[0^o/90_i{}^o/0^o]_{10T}$ means that there is a stacking which consists of one thickness of 0^o, i thicknesses of 90^o and one thickness of 0^o, and repeated ten times.

Results obtained for symmetric cross-ply delaminated plates are similar to those for the orthotropic plate.

Table 9 shows the values of the buckling loads, $\bar{P}$, of a clamped symmetric cross-ply with stacking sequence $[0^o/90^o/10^o]_{10T}$, for several values of the delamination length parameter $\bar{a}$, and of the delamination thickness prameter, $\bar{h}$. The same results are shown graphically in Fig. 7. The results show that for a relatively thin delaminatin ($\bar{h} \leq .2$), the presence of delamination has a negligible effect on the buckling load of the delaminated plate, as long as $\bar{a} \leq \bar{h}$. On the other hand, for the case where $\bar{a} > \bar{h}$ the value of the buckling loads is greatly affected by the presence of delamination, especially for plates with thin delamination.

Tables 10 and 11 show similar results for the same configuration but with stacking sequence $[0^o/90^o_2/0^o]$ and $[0^o/90^o_4/0^o]$ respectively. The results of Tables 9, 10 and 11 are compared graphically in Fig. 8, with the results obtained previously for the orthotropic plate (Table 1) for delaminatin thickness $\bar{h}$ =.1.

It is clear from Fig 8. that as the thickness of the 90^o layers increases w.r.t. the thickness of the 0^o layers the value of the buckling load parameter becomes larger for the same delamination length and thickness. On the other hand, we have to realize that the value of the

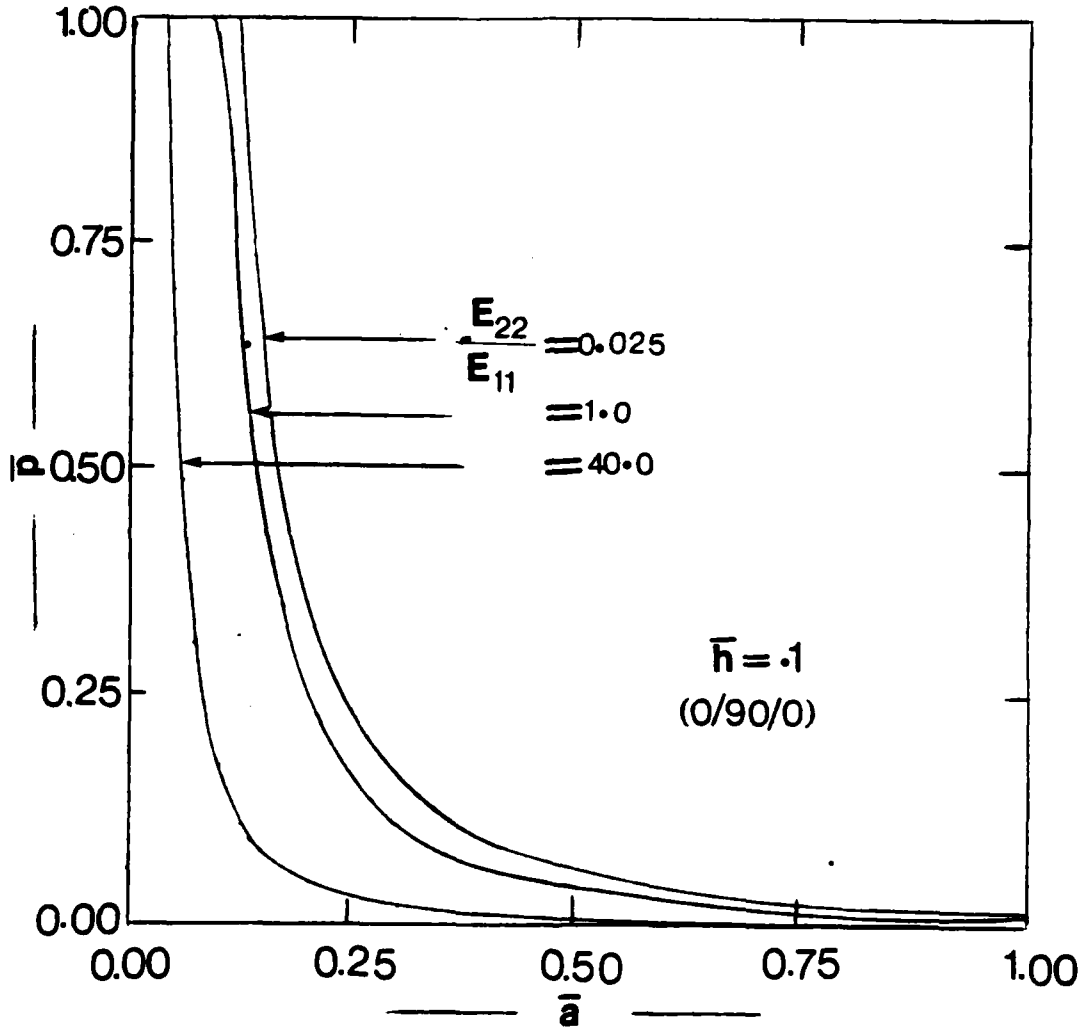

Fig. 9 Effect of relative stiffness on the buckling load of symmetric cross-ply laminates.

Table 12. Buckling Loads for Symmetric Cross-ply Laminates, $[0^{\circ}/90^{\circ}_{2}/0^{\circ}]_{10T}$, with Simply Supports Ends.

$\frac{h}{a}$	.1	.2	.3	.4	.5
0.05	.9999995	.9999997	.9999998	.9999998	.9999998
0.10	.9999814	.9999873	.9999903	.9999917	.9999921
0.15	.9998244	.9998977	.9999250	.9999364	.9999396
0.20	.9986462	.9995297	.9996747	.9997290	.9997439
0.25	.9856249	.9983632	.9989669	.9991611	.9992122
0.30	.7493109	.9950259	.9972902	.9978754	.9980213
0.40	.4231350	.9511346	.9866541	.9906448	.9914956
0.50	.2710060	.7105996	.9483680	.9701004	.9738030
0.60	.1882612	.5026573	.8406581	.9239711	.9364303
0.70	.1383413	.3715466	.6816561	.8435466	.8742498
0.80	.1059314	.2853457	.5420407	.7385384	.7923643
0.90	.0837068	.2258895	.4362642	.6313119	.7033758
1.00	.0678074	.1832116	.3572710	.5363347	.6181324

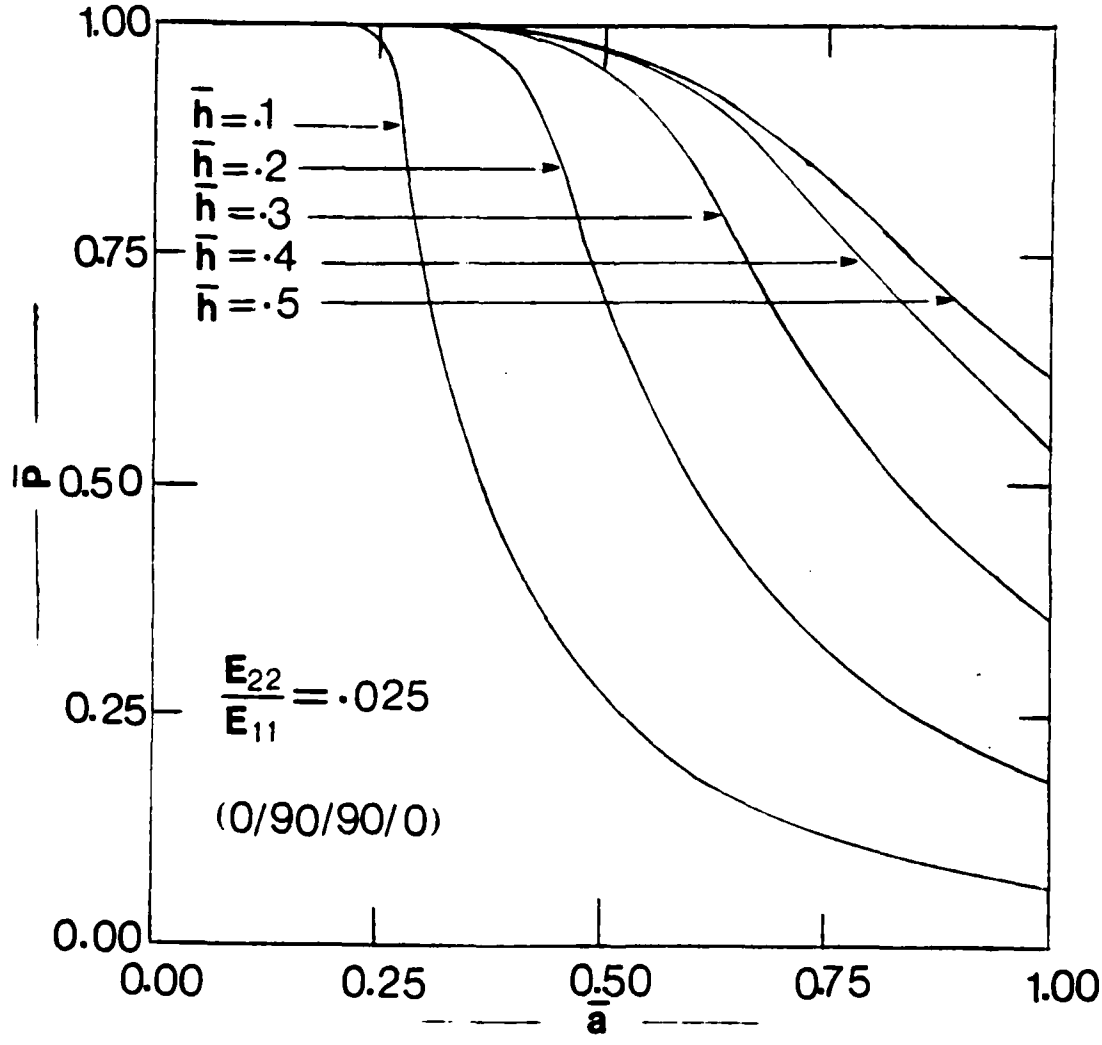

Fig. 10 Effect of Symmetric Delamination on Buckling Loads of Cross-Ply Laminates with Simply Supported Ends.

buckling load parameter for each case is normalized w.r.t. the perfect configuration.

The effect of relative value of transverse modulus (E_{22}) to the tensile modulus (E_{11}) is studied. Fig. 9 illustrates this effect for the case of a symmetric, delaminated, cross-ply plate with clamped-clamped boundary condition for a delamination thickness parameter $\bar{h} = .1$. The considered cross-ply plate has stacking sequence $[0/90/0]_{10T}$. The results show that when the 0^o layers and 90^o layers are interchanged, the buckling load parameter drops drastically even for $\bar{a} < \bar{h}$. A similar result has been obtained for a $[0^o/90^o/0^o]_{10T}$ cross-ply laminate with simply supported boundary conditions. These results are presented on Table 12 and in Fig. 10. The results of this case are similar to those of the orthotropic plate in general, but it is noticed that for relatively thin delamination ($\bar{h} = .1$) the buckling load parameter for the cross-ply laminate is much higher than that of the orthotropic plate. This difference becomes smaller as the delamination thickness increases.

III.1.3 Conclusions

A simple model has been employed to study delamination buckling and the effect of location, size, and thickness of delamination on the buckling load. The simplicity of the model limits the applicability of the results to the case for which each region of the four parts of the plate is symmetric w.r.t its reference plane.

For these geometries (laminates) the results serve a different purpose. They can be employed to relate the ultimate load carrying capacity of the completely (throughout) damaged laminate to the allowable for the delaminated laminate.

A good application of the present analysis and results is in the analysis of adhesive bonding of two similar materials [1].

III.2 Delamination Growth Results

First of all, before presenting any results, we are goint to illustrate the growth mechanism of the delaminated laminate, let us consider Fig. 11. Consider a material with critical fracture toughness $\bar{G}^*$ and initial delamination length $\bar{a}_o$. The load is increased quasistatically to $\bar{p}_o$, where the critical value of the energy release rate, $\bar{G}^*$, is reached. As the delamination length extends by an amount $\Delta\bar{a}$, while the load is kept constant, the figure shows that the available energy release rate corresponding to the new delamination length $\bar{a} + \Delta\bar{a}$, exceeds the critical value $\bar{G}^*$, hence growth will take place. On the other hand, if the initial delamination length is $\bar{a}_1$, in this case an increase in the delamination length $\Delta\bar{a}_1$, will result in a decrease in the energy release rate, consequently there will be no delamination growth as long as the load does not changed (increased).

III.2.1 Orthotropic Plate:

Figures 12 to 14 contain three sets of curves showing the relations between the non-dimensionalized eneryg-release rate, $\bar{G} = L^4G/(Et^5)$, and the normalized delamination length $\bar{a} = a/L$, under fixed axial load and delamination thickness. The three figures correspond respectively to the cases $\bar{h} = 0.2$, 0.1 and 0.02. These values of the normalized thickness are thought to be representative of relatively thick, a relatively thin, and an extremely thin delamination. Each curve in these figures refers to a fixed value of the normalized axial load $\bar{P}$, and each curve is obtained from a one-parameter family of numerical solutions of Eq. (75). In the case of relatively long delaminations ($\bar{a}/\bar{h} > 1$), $\bar{G}$ varies over a wide range of

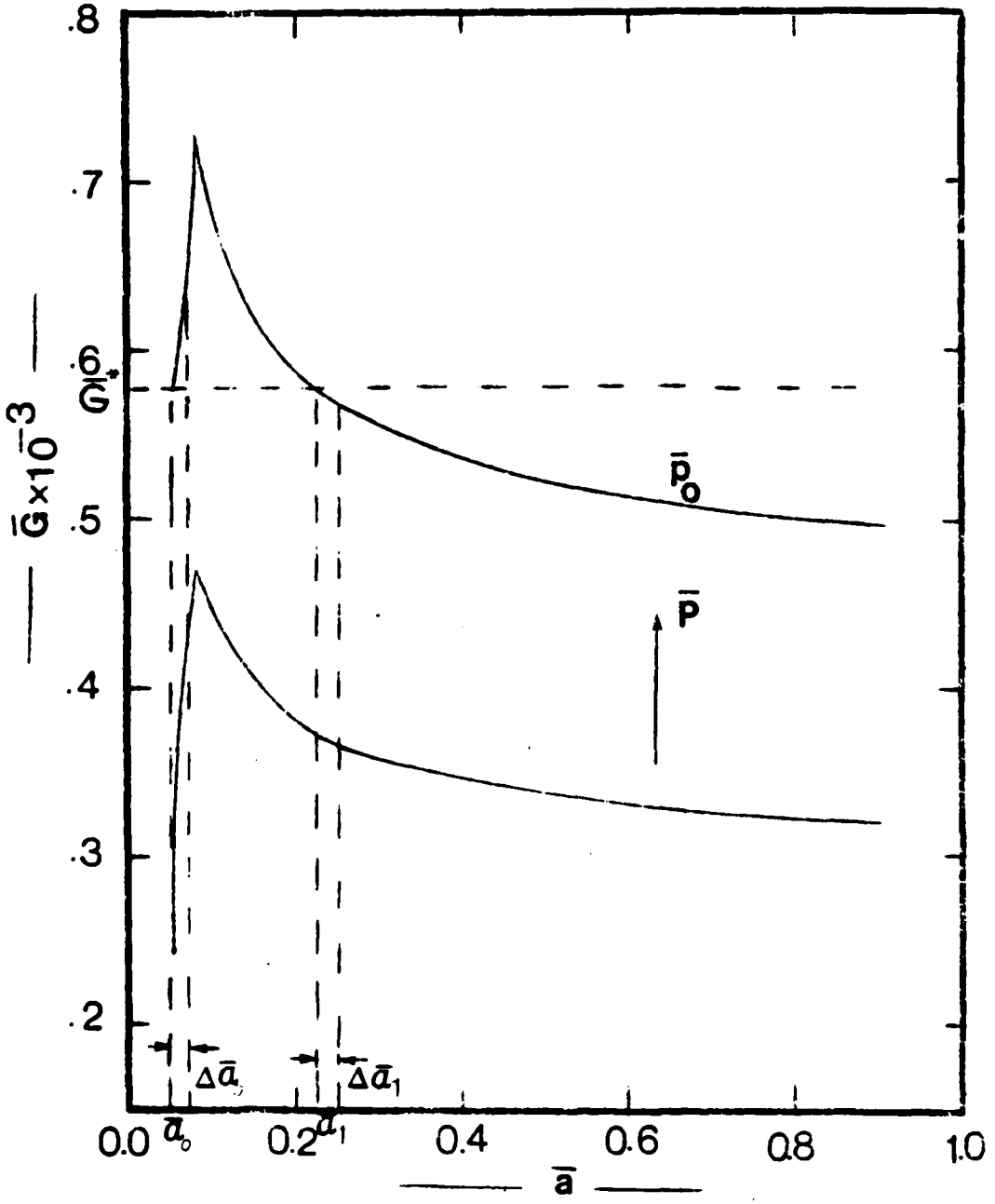

Fig. 11 Energy Release Rate vs Delamination Length

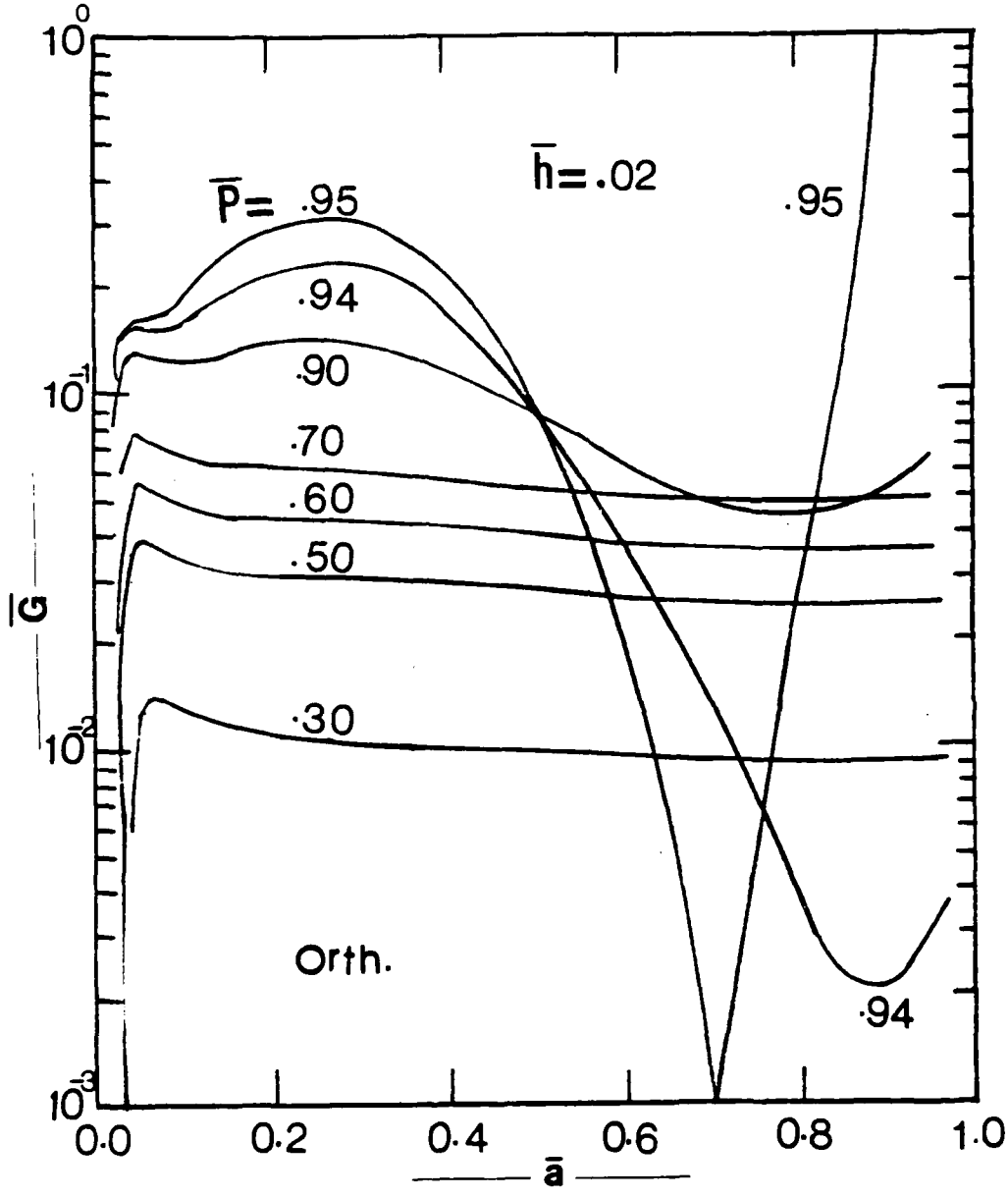

Fig. 12 Energy Release Rate for Orthotropic Plate

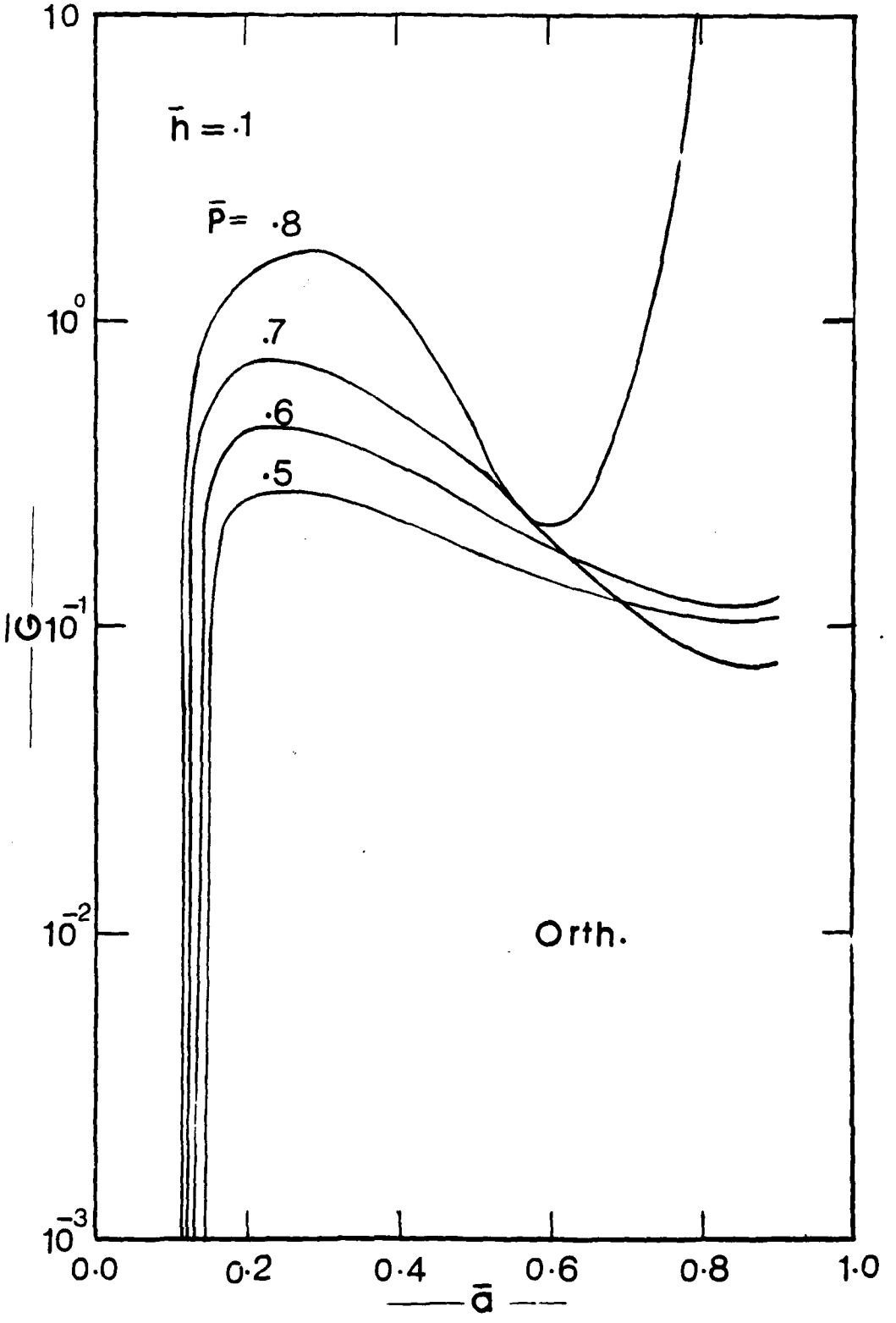

Fig. 13 Energy Release Rate for Orthotropic Plate

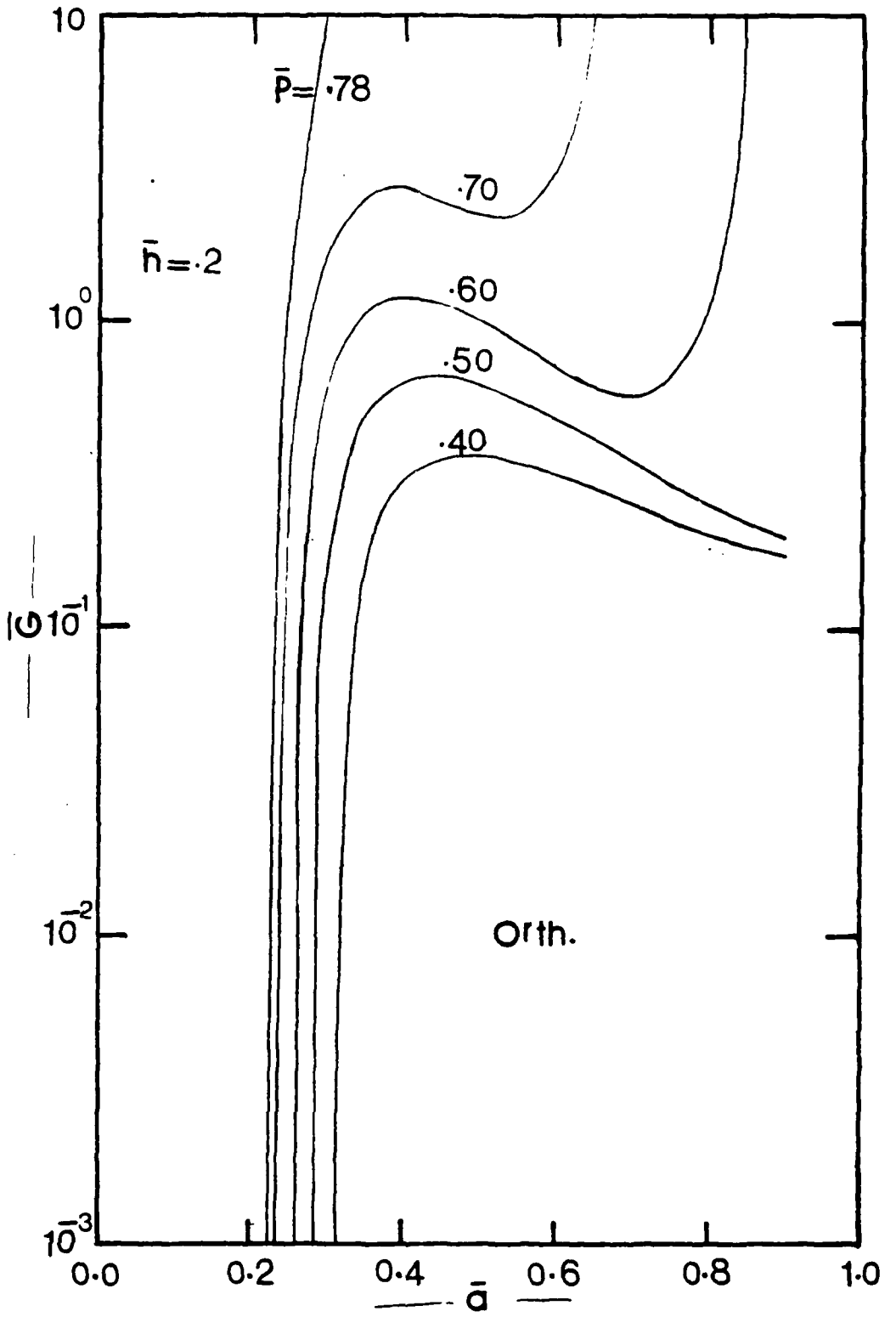

Fig. 14 Energy Release Rate for Orthotropic Plate

values as $\bar{a}$ changes. Hence the curves are plotted in a semi-logrithmic diagram.

In a quasi-static process of delamination growth, the energy-release rate $\bar{G}$ maintains a constant critical value $\bar{G}^*$ (the non-dimensionalized fracture toughness).

Figures 12-14 show that if the fractue toughness is relatively small, say $\bar{G}^* < 10^{-2}$ (for very thin delamination $\bar{h} = .02$) and $\bar{G}^* < 10^{-1}$ (for $\bar{h} \geq .1$), then the delamination growth is unstable, in general, although it may become stable shortly before the state of complete delamination ($\bar{a} = 1$). Hence, if $\bar{G}^*$ is small, delamination growth under a constant axial load $\bar{P}$ (a dead load) is generally a catastrophic process. When a delaminated plate buckles under an increasing axial load $\bar{P}$, the postbuckling solution follows a vertical path on the $\bar{G}$-$\bar{a}$ curves ($\bar{a}$ = constant) until the curve intersects the horizontal path $\bar{G} = \bar{G}^*$. The value of $\bar{P}$ at the intersecting point is the ultimate axial load capacity of the plate. Afterwards delamination growth starts and proceeds catastrophically under a constant axial load.

If the length of existing delamination is relatively short ($\bar{a} < \bar{h}$), then $\bar{G}$ never attains the critical value $\bar{G}^*$ and, consequently, delamination growth does not occur. For such plates, the ultimate axial load capacity is not governed by delamination growth, but is determined by its elastic postbuckling behavior. The critical buckling load is a lower bound of , and a close estimate for, the ultimate axial load capacity.

If the fracture toughness is relatively large, say $\bar{G}^* > .3$ (for very thin delaminatin, $\bar{h} = .02$) and $\bar{G}^* > 1.$ (for $\bar{h} \geq .1$), the figures show that all curves lie above the curve corresponding to $\bar{P}_{dam}$ ($\bar{P}_{dam} = \bar{h}^3 + (1-\bar{h})^3$). Consequently, if $\bar{h}$ is small and $\bar{G}$ is large (as given above), the critical (buckling) load of a completely delaminated plate is a close lower bound of

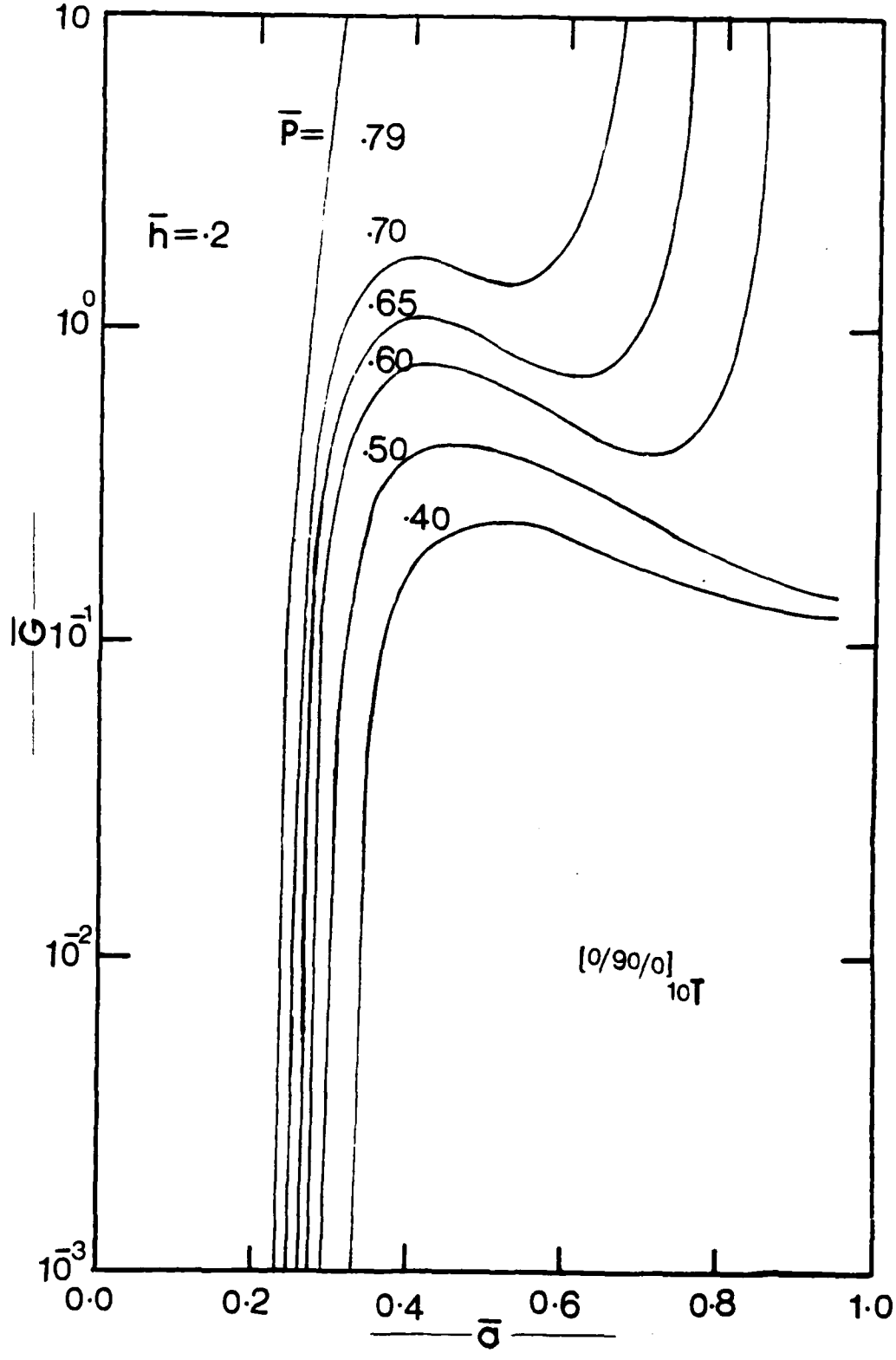

Fig. 15 Energy Release Rate for Symmetric Cross-ply Laminates

the ultimate load carrying capacity of the laminate. If the fracture toughness lies between these two extreme cases, rel tively high and relatively low, then the delamination growth and the load carrying capacity will depend upon the value of the fracture toughness $\bar{G}^*$ as well as on the initial delamination length parameter. The above statement is true as long as the deflection and the end shortening are both bounded (see Figures 18 and 19). It is clear from the obtained results that for the same level of the applied load and for the same delamination length, the energy release rate increases as the delamination thickness increases, i.e. for the same material the possibility of delamination growth increases as the thickness of the delamination increases.

III.2.2 Symmetric Cross-Ply Plate

The energy release rate is obtained for a delaminated plate made up of Graphite/Epoxy with same material constants as given in the results of the buckling problem. Among the different stacking sequence configurations, which we deal with in the buckling problem, we are going to consider the case of the stacking sequence $[0^o/90^o/0^o]_{10T}$. Fig. 15, shows the results for the cross-ply laminate with delamination thickness $\bar{h} = .2$. The general shape of the obtained curves is similar to that of the orthotropic plate. The only difference between the cross-ply results and the orthotropic results is that for the same delamination length and delamination thickness and some applied load, the energy release rate for the cross-ply laminate is smaller (not much) than that of the orthotropic plate. Note that, when we say same level of the applied load, we have to keep in mind that this load is normalized w.r.t. the perfect geometry plate in each case.

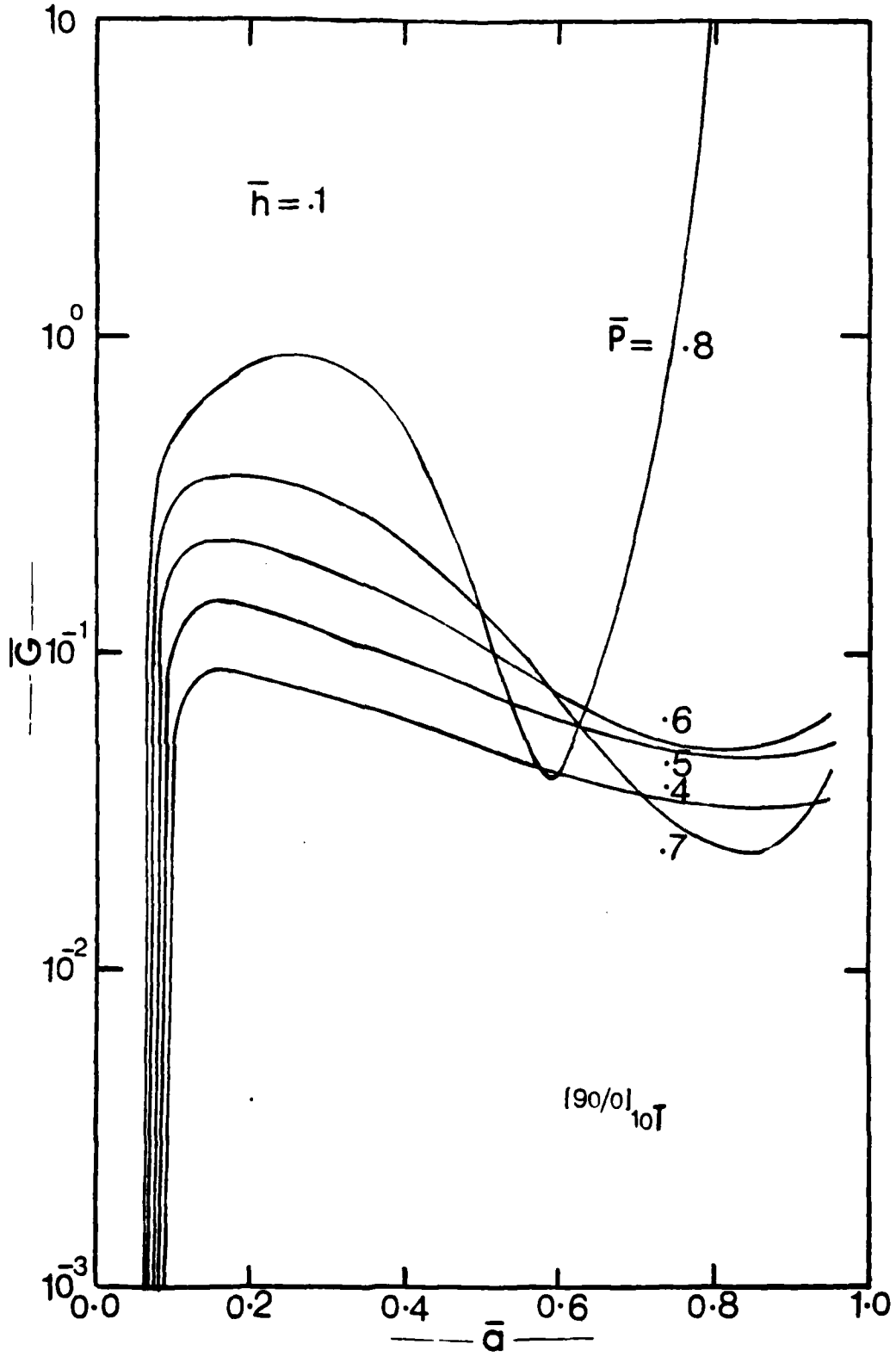

Fig. 16 Energy Release Rate for Unsymmetric Cross-ply Laminates

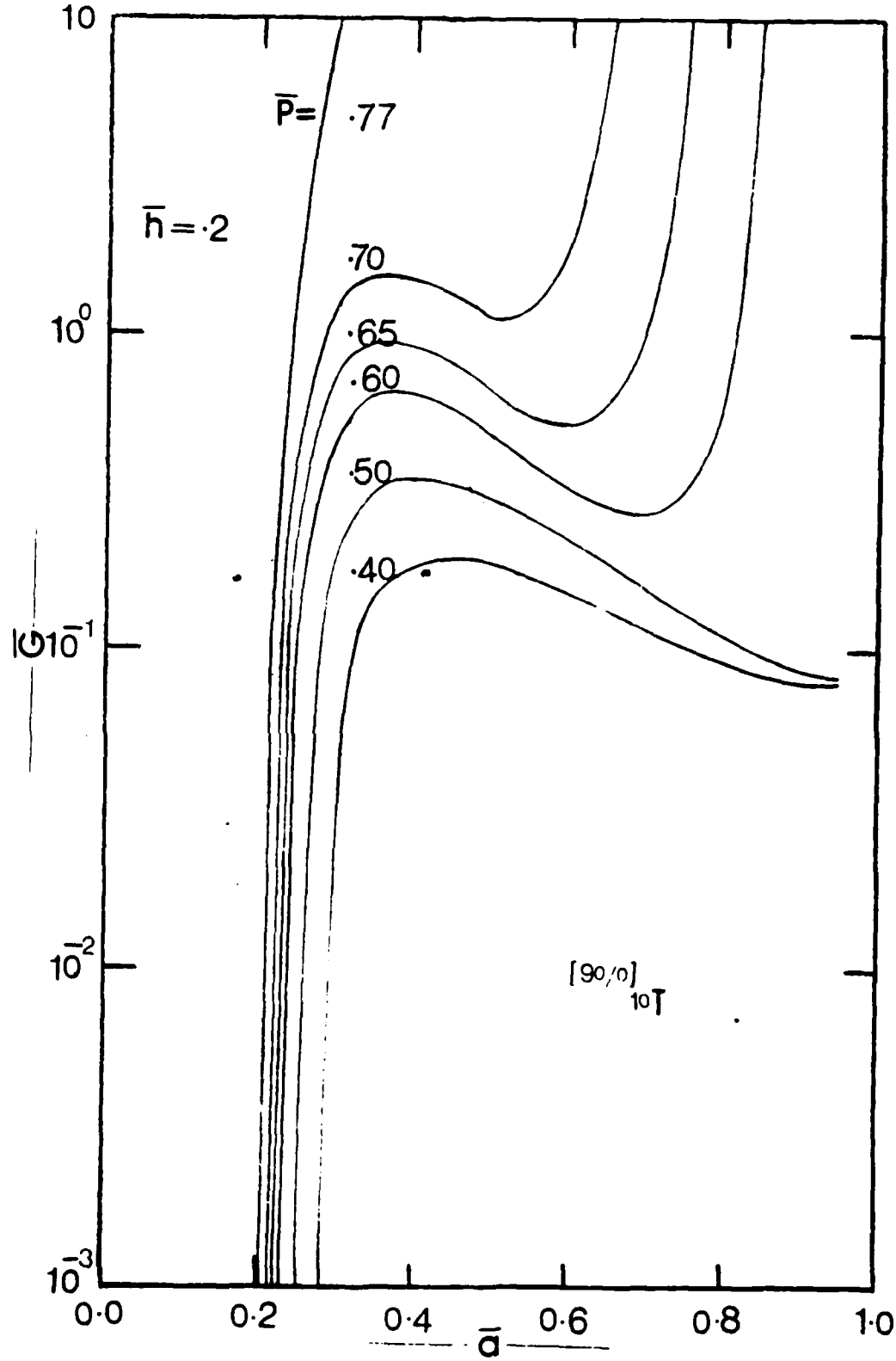

Fig. 17 Energy Release Rate for Unsymmetric Cross-ply Laminates

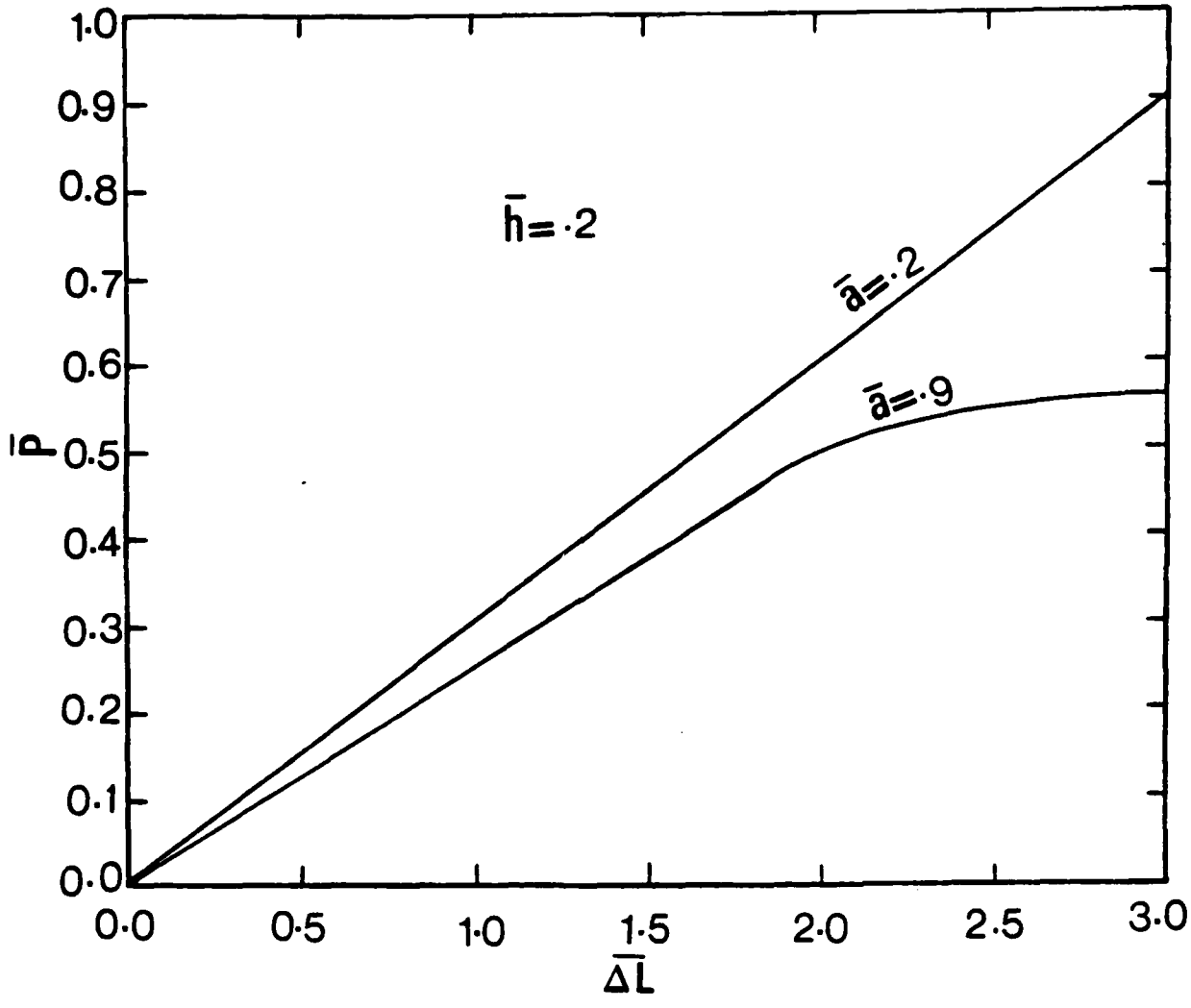

Fig. 18 End shortening of delaminated orthotropic plate.

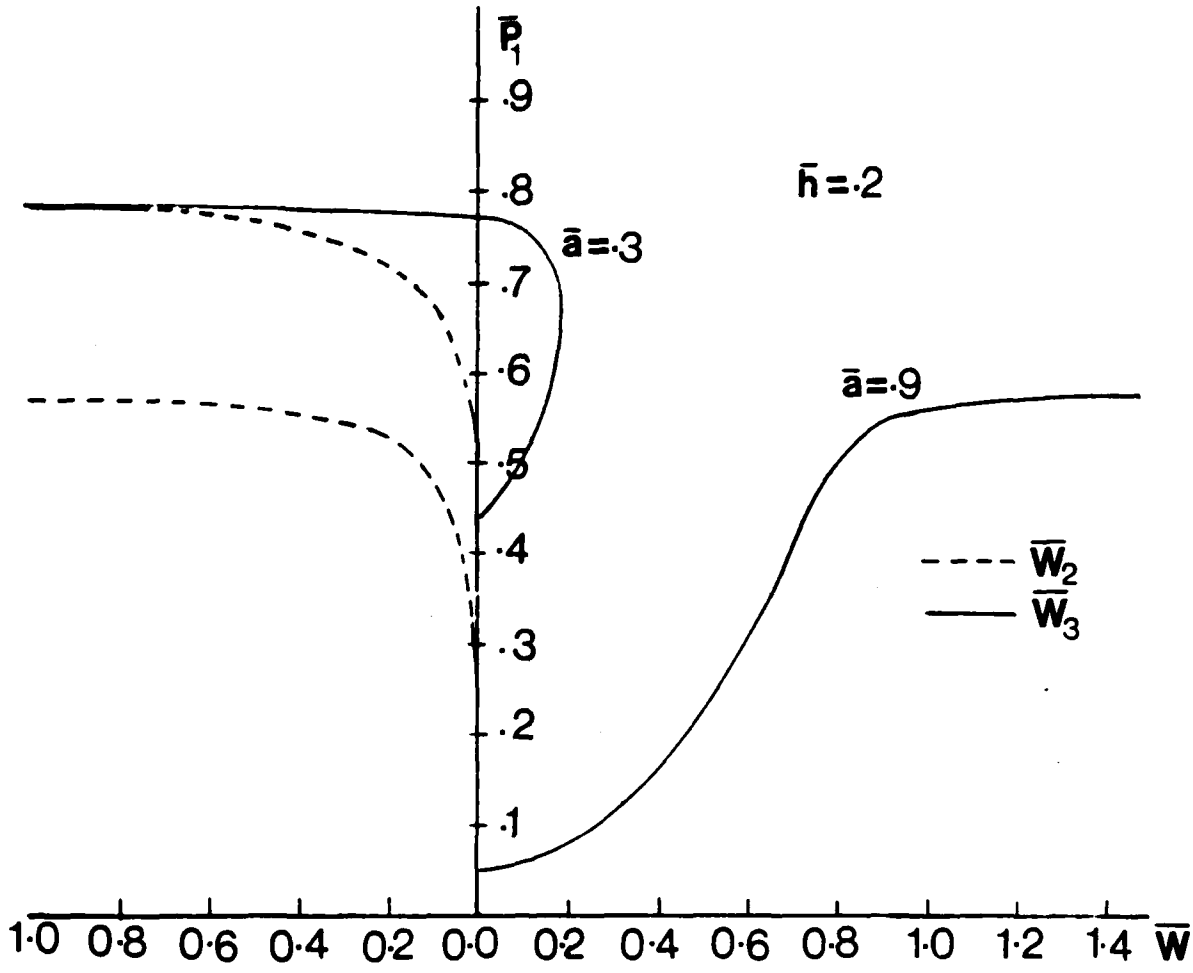

Fig. 19 Deflection of mid-point of delaminated orthotropic plate.

III.2.3 Unsymmetric Cross-ply

Since for laminates, in general, there exists a coupling between bending ane extension, the present model is used to study the effect of the presence of coupling between bending and stretching on delamination growth. In this aspect, a delaminated plate in the form of unsymmetric cross-ply laminate is studied. Note that for such geometry, there is coupling between bending and stretching regardless of the level of the applied load, and therefore the possibility of bifurcational buckling does not exist. The unsymmetric cross-ply, $[90^{o}/0^{o}]_{10T}$ is made up of Graphite/Epoxy. Figs. 16 & 17 show the energy release rate vs the delamination length for various levels of the applied loads for delamination thickness $\bar{h} = .1$ and $\bar{h} = .2$, respectively. Unlike the orthotropic case, Fig. 16 shows that even for $\bar{a} < \bar{h}$ there exist an energy release rate, and the curves suggest unstable growth in this range. The results show that for the same parameters, the energy release rate for the unsymmetric cross-ply is less than that of the orthotropic plate. Fig. 17 gives the energy release rate for the unsymmetric cross-ply with delamination thickness $\bar{h} = .2$, the results are similar to that obtained for the orthotropic and (symmetric) cross-ply plate.

REFERENCES

1. Chow, C. L. and Ngan, K. M. "Method of Fracture Toughness Evaluation of Adhesive Joints" J. Strain Analysis, Vol. 15, No. 2, 1980 pp. 97-101.

2. Chai, H. Ph.D. Thesis, "The Growth of Impact Damage in compressively loaded laminates", California Institute of Technology, Pasadena, California, 1982.

3. Whitcomb, J. D. "Approximate Analysis of Postbucling Through-Width Delamination", NASA Technical Memorandum TM-83147 (1981).

4. Whitcomb, J. D. "Finite Element Analysis of Instability Related Delamination Growth", J. Comp. Materials, Vol. 15, 1981, pp. 403-426.

5. Yin, W. L., and Wang, J. T. S. "Postbuckling Growth of a One-Dimensional Delamination. Part-I Evaluation of the Energy Release Rate", J. Appl. Mechanics, Submitted for Publication, 1983.

6. Konishi, D. Y. and Johnston, W. R. "Fatigue Effects of Delamination and Strength Degradation in Graphite/Epoxy Laminates", Composite Materials: Testing and Design (fifth Conference), ASTM STP 674, S. W. Tsai, Ed. 1979, pp. 597-619.

7. Yin, W.L. "Axisymmetric Buckling and Growth of a Circulr Delamination in a Compressed Laminate", Int. J. Solids and Structures, Submitted for Publication, 1983.

8. Bottega, W. J. and Maewal, A. "Delamination Buckling and Growth in Laminates", J. Appl. Mechanics, Vol. 50, No. 1, 1983, pp. 184-189.

9. Bottega, W. J. and Maewal, A. "Dynamics of Delamination Buckling", Proceedings of AIAA/ASME/ASCE/AHS 24th SDM Conference, Paper 83-0873 Lake Tahoe, Nevada May 1983.

10. Shivakumar, K. N. and Whitcomb, J. D. "Buckling of a Sublaminate in a Quasi-Isotropic Composite Laminate" NASA, TM-85755 (1984).

11. Brogan, F. A. and Almroth, B. O. "Buckling of Cylinders with Cutouts", AIAA J., Vol. 8, 1970, pp. 236-260.

12. Meller, E. and Bshnell, D. "Buckling of Steel Containment Shells" Lockheed Palo Alto Research Labs, CA, CR-7863 (Dec. 1982).

13. Baker, w. and Bennet, J. "Buckling Investigation of Ring-Stiffened Cylindrical Shells with Reinforced Openings under Unsymmetrical Axial Loads" Los Alamos National Laboratory report LA-9646-MS (Feb. 1983).

14. Byers, B. A. "Behavior of Damaged Graphite/Epoxy Laminates under Compression Loading", NASA CR-159293 (August 1980).

15. Eshelby, J. D. "The Determination of the Elastic Field of an Ellipsoidal Inclusion, and Related Problems" Proceedings Roy. Soc., Series A, Vol 241, London, 1957, pp. 376-396.

16. Walpole, L. J., "The Elastic Field of an Inclusion in an Anisotropic Medium", Proceedings Roy. Co., Series A, Vol. 300, London 1967, pp. 270-289.

17. Van Dyke, P., "Stress in a Cylindrical Shell with A Rigid Inclusion" AIAA J., Vol. 5, No. 1, Jan. 1967, pp. 125-137.

18. Kinoshita, N., and Mura, T., "Elastic Fields of Inclusions in Anisotropic Media" Physica Status Solidi, Vol. (a)5, 1971, pp. 759-768.

19. Takao, Y., Taya, M., and Chou, T. W., "Stress Field Due to a Cylindrical Inclusion with Constant Axial Eigenstrain in an Infinite Elastic Body" J. Appl. Mech., Vol. 48, No. 4, 1981, pp. 853-858.

20. Kulkarni, S. V. and Frederick, D. "Buckling of Partially Debonded Layered Cylindrical Shells", Proceedings of AIAA/ASME/SAE 14th SDM Conference, Williamsburg, Virginia, March 1973.

21. Jones, R. M. "Buckling of Stiffened Two-Layered Shells of Revolution with a Circumferentially Cracked Unbonded Layer", AIAA J. Vol. 7, 1969, pp. 1511-1517.

22. Troshin, V. P., "Effect of Longitudinal Delamination in a Laminar Cylindrical Shell on the Critical External Pressure", J. of Comp. Materials, Vol. 17, No. 5, 1983, pp. 563-567.

23. Bellman, R., Perturbation Techniques in Mathematics, Physics and Engineering, Holt, Rinehart and Winston, New York, New York, 1969.

24. Sewell, M. J., "The Static Perturbation Technique in Buckling Problems" J. Mech. and Phys. of Solids, Vol. 13, 1965, pp. 247-254.

25. Simitses, G. J., Elastic Stability of Structures, Prentice-Hall Inc., Englewood Cliffs, N.J., 1976 (Ch. 7).

26. Calcote, L. R. "The Analysis of Laminated Composite Structures", Van Nostrand Reinhold Company, New York, 1969 (Ch. 6).

27. Rice, J. R. "A Path Independent Integral and the Approximate Analysis of Strain Concentration by Notches and Cracks", J. Appl. Mech. 1968 pp. 379-386.

28. Brock, D., Elementary Engineering Fracture Mechanics, Martinue Nijhoff Publishers, 1982 (Ch. 5).

29. Whitcomb, T. D. "Strain Energy Release Rate Analysis of Cyclic Delami nation Growth in Compressively Loaded Laminates" NASA Technical memorandum 84598 (Jan., 1983).

END

FILMED

1-86

DTIC